

Comparison of Q-estimation methods: an update

Peng Cheng and Gary F. Margrave

ABSTRACT

In this article, three methods of Q estimation are compared: a complex spectral ratio method, the centroid frequency-shift method, and a time-domain match-filter method. Their performance for Q estimation is evaluated using synthetic data and real data in terms of accuracy and robustness to noise. Testing results shows that the complex spectral-ratio method, with phase information employed, can obtain improved estimation results. The centroid frequency-shift method is robust to noise and gives stable estimations, while the accuracy of estimated result is subject to the frequency band used to estimate centroid frequency and variance. The match-filter method is robust to noise and can give accurate estimation result for both VSP data and reflection data.

INTRODUCTION

There are various methods for Q estimation such as analytical signal method (Engelhard, 1996), spectral-ratio method (Bath, 1974), the centroid frequency-shift method (Quan and Harris, 1997), the match-technique method (Raikes and White, 1984; Tonn, 1991), and the spectrum-modeling method (Janssen et al., 1985; Tonn, 1991; Blias, 2011), and each method has its strengths and limitations. An extensive comparison between various methods for Q estimation was made by Tonn (1991) using VSP data, and a conclusion was made that the spectral-ratio method is optimal in the noise-free case. However, the estimation given by spectral-ratio method may deteriorate drastically with increasing noise (Patton, 1988; Tonn, 1991). The question of reliable Q estimation remains.

As an extension to classic spectral-ratio method, Cheng and Margrave (2008) propose a complex spectral-ratio method that employs both the amplitude spectra and the phase spectra of signal, in which Q is estimated by solving an inverse problem to minimize the misfit between the modeled and measured complex spectral ratios. In addition, Cheng and Margrave (2012a) propose a time-domain match-filter method for Q estimation, which has been shown to be robust to noise and suitable for application to surface reflection data. Theoretically, the match-filter method is a sophisticated wavelet-modeling method, which is a time-domain alternative to spectrum-modeling method (Janssen et al., 1985; Tonn, 1991; Blias, 2011). The spectrum-modeling method is a modified approach to the spectral-ratio method without taking division of spectra. In addition, the match-filter method and the match-technique method (Raikes and White, 1984; Tonn, 1991) employ the idea of matching at different stages of their Q-estimation procedures. Therefore, the above four methods all have theoretical connections but are distinctly different. Cheng and Margrave (2012b) give a comparison of these methods using synthetic VSP and reflection data and real VSP data and show that the match-filter method has superior performance.

The purpose of our work is to, as an update to our work (Cheng and Margrave, 2012b), compare three Q-estimation methods including complex spectral-ratio method, centroid

frequency-shift method and match-filter method. This paper is organized as follows: the first part introduces the basic theory of the three methods. Then, some numerical examples will be used to evaluate their performance. Finally, some conclusions are made based on the testing results.

THEORY OF Q-ESTIMATION METHODS

The theory of the constant Q model for seismic attenuation is well established (Futterman, 1962; Aki and Richards, 1980). Suppose that a seismic wavelet with amplitude spectrum $|S_1(f)|$ has a amplitude spectrum $|S_2(f)|$ after traveling in the attenuating media for an interval time t . Then, we have

$$|S_2(f)| = G|S_1(f)| \exp\left(\frac{-\pi ft}{Q}\right), \quad (1)$$

where f is the frequency, G is a geometric spreading factor. More generally, G can represent all the frequency independent amplitude loss in total, including spherical divergence, reflection and transmission loss.

For Q estimation, the case of VSP data is similar to the case of reflection data with isolated reflectors. So, we use the reflection data to form the Q -estimation problem. Assume that a source wavelet $s(t)$ with a spectrum $S(f)$ travel through layered earth with a corresponding reflectivity $r(t)$ in two way time, and $g(t)$ denotes the geometric spreading loss of amplitudes. Then, for an acoustic/elastic medium, the reflected signal $a(t)$ can be given by

$$a(t) = g(t) \int_{-\infty}^{\infty} s(\gamma) r(t - \gamma) d\gamma. \quad (2)$$

Consider a locally reflected wave $a_1(t)$, i.e. a windowed part of $a(t)$ has the contribution from a corresponding subset of reflectivity, $r_1(t)$, which is around two way time t_1 . From (2), we have

$$a_1(t) \approx g(t_1) \int_{-\infty}^{\infty} s(\gamma) r_1(t - \gamma) d\gamma. \quad (3)$$

Then the spectrum of the localized signal $a_1(t)$ near time t_1 can be approximated by

$$A_1(f) \approx g(t_1)S(f)R_1(f), \quad (4)$$

where $R_1(f)$ is the Fourier transform of $r_1(t)$ and we assume $g(t)$ changes slowly with respect to $s(t)$. If the attenuation of the layered medium is taken into account and the attenuation mechanism can be described by the constant Q model, equation (4) should be modified as

$$|A_1(f)| \approx g(t_1)|S(f)||R_1(f)| \exp\left(\frac{-\pi ft_1}{Q}\right). \quad (5)$$

Similarly, for a localized reflected signal $a_2(t)$ near time t_2 with a corresponding local reflectivity series $r_2(t)$, we have

$$a_2(t) \approx g(t_2) \int_{-\infty}^{\infty} s(\tau) r_2(t - \tau) d\tau. \quad (6)$$

when attenuation is taken into account, its amplitude spectrum of $a_2(t)$ can be formulated as

$$|A_2(f)| \approx g(t_2) |S(f)| |R_2(f)| \exp\left(\frac{-\pi f t_2}{Q}\right), \quad (7)$$

where $R_2(f)$ is the Fourier transform of $r_2(t)$.

Actually, for absorptive media, the $s(\tau)$ term in equation (3) and (6) should be replaced by their corresponding evolving version $s_1(\tau)$ and $s_2(\tau)$. There are various methods for Q estimation, in which Q is usually derived from the local waves $a_1(\tau)$, $a_2(\tau)$ or their spectra. We will discuss different methods for Q estimation based on the model of local waves given in equation (3), (5), (6) and (7).

Complex spectral-ratio method

The classic spectral-ratio method is commonly used to estimate Q from VSP data. However, this method only uses the amplitude spectra of the downgoing wavelets. Cheng and Margrave (2008) investigate a complex spectral-ratio method, in which both amplitude spectrum and phase spectrum are employed to obtain improved estimation of Q. The complex spectral-ratio between the two wavelets in equation (3), (6) can be expressed in frequency domain as (Cheng and Margrave, 2008)

$$\ln \left[\frac{A_2(f)}{A_1(f)} \right] \approx -\frac{\pi f \tau}{Q_{int}} + b + j \left[\frac{2f\tau}{Q_{int}} \ln \left| \frac{f}{f_0} \right| \right], \quad (8)$$

where Q_{int} is the interval-Q value, τ is the interval travel time between the two local wavelets, and b is a constant term representing the frequency independent energy loss.

For the classic spectral-ratio method (Spencer et al., 1982), only the real part of spectral ratio in equation (8) is considered, and Q can be estimated by fitting a straight line to the calculated spectral ratios. Either the least-squares (L_2 norm) solution or the L_1 norm solution can be chosen for straight-line fitting. Then, Q can be estimated as

$$Q_{est} = -\frac{\pi\tau}{k}, \quad (9)$$

where k is the slope of the straight line fitted to the real part of calculated spectral ratios.

Now, we will use the complex spectral ratios to conduct Q estimation. Suppose that N complex spectral ratios are obtained for frequency components f_1, f_2, \dots, f_N . Let R_e , I_m , M_1 and M_2 be the column vectors with N elements expressed as

$$\begin{cases} Re = \left[Re \left(\ln \left[\frac{A_2(f_1)}{A_1(f_1)} \right] \right), Re \left(\ln \left[\frac{A_2(f_2)}{A_1(f_2)} \right] \right), \dots, Re \left(\ln \left[\frac{A_2(f_N)}{A_1(f_N)} \right] \right) \right]^T \\ Im = \left[Im \left(\ln \left[\frac{A_2(f_1)}{A_1(f_1)} \right] \right), Im \left(\ln \left[\frac{A_2(f_2)}{A_1(f_2)} \right] \right), \dots, Im \left(\ln \left[\frac{A_2(f_N)}{A_1(f_N)} \right] \right) \right]^T \\ M_1 = [-\pi f_1 \tau, -\pi f_2 \tau, \dots, -\pi f_N \tau]^T \\ M_2 = \left[-2f_1 \tau \cdot \ln \left| \frac{f_1}{f_0} \right|, -2f_2 \tau \cdot \ln \left| \frac{f_2}{f_0} \right|, \dots, -2f_N \tau \cdot \ln \left| \frac{f_N}{f_0} \right| \right]^T \end{cases} \quad (10)$$

Then, equation (8) can be rewritten as

$$R_e + iI_m = M_1 m + E_N b + iM_2 m, \quad (11)$$

where E_N is a column vector with N unit elements, m is the reciprocal of Q_{int} , i.e

$$Q_{int} = 1/m. \quad (12)$$

Therefore, Q can be obtained by solving the forward model

$$L \mathbf{m} = D, \quad (13)$$

where L is a matrix given as

$$L = \begin{bmatrix} M_1 & E_N \\ M_2 & 0 \end{bmatrix}, \quad (14)$$

and \mathbf{m} is a vector of that only contains parameter m and b . Then, the least-squares solution for equation (13) can be formulated as

$$\hat{\mathbf{m}} = (L^T L)^{-1} L^T D. \quad (15)$$

Equation (15) shows one way to combine amplitude spectrum and phase spectrum to give Q estimation. The contributions from amplitude spectrum and phase spectrum might be unbalanced. To address this issue, matrix L and vector D in equation (13) can be modified as

$$\hat{L} = \begin{bmatrix} \varepsilon M_1 / e_1 & E_N / e_1 \\ (1 - \varepsilon) M_2 / e_2 & 0 \end{bmatrix}, \quad (16)$$

and

$$\hat{D} = \begin{bmatrix} \varepsilon R_e / e_1 \\ (1 - \varepsilon) I_m / e_2 \end{bmatrix}, \quad (17)$$

where ε is a scaling factor between 0 and 1, and can be given manually, e_1 and e_2 are the least-squares errors when only amplitude spectrum or phase spectrum is employed for the Q estimation. Then, the least-squares solution to the alternative of equation (3.29) can be formulated as

$$\hat{\mathbf{m}} = (\hat{L}^T \hat{L})^{-1} \hat{L}^T \hat{\mathbf{D}}. \quad (18)$$

The result in equation (18) is a generalized complex spectral-ratio method. The contribution to estimation result from amplitude spectrum information and phase spectrum information is normalized, and can be adjusted by changing the scaling factor ε . It reduces to the classic spectral-ratio method when $\varepsilon = 1$, and uses phase information only to conduct Q estimation when $\varepsilon = 0$.

The complex spectral-method described above is developed only for VSP data. Theoretically, the estimation result varies with reference frequency f_0 . In addition, the two wavelets used to conduct Q estimation should be aligned properly to minimize the linear phase shift. When applied to real data, a practical but important issue for the complex spectral-ratio method is that an appropriate reference frequency f_0 should be determined first to model the phase difference between the local wavelets, since there is no relevant prior knowledge available. For real VSP data with good quality, the Q estimation based on phase information only should obtain a result that is similar to the result given by classic spectral-ratio method. This criterion can be used to roughly choose the reference frequency. An alternative approach can be that f_0 is determined by minimizing the mismatch between modeled phase difference and measured phase difference. Another approach can be that minimum-phase equivalent wavelets are computed for the two original wavelets to conduct subsequent Q -estimation, then f_0 can be chosen with the calibration from other Q -estimation methods. These three approaches will be investigated using real VSP data.

Centroid frequency-shift method

A frequency-shift method for estimating seismic attenuation is introduced by Quan and Harris (1997). The $|A_1(f)|$ and $|A_2(f)|$ in equation (5) and (7) can be taken as the amplitude spectra of input signal and output signal for an attenuation process respectively. The centroid frequency for the input signal can be defined as (Quan and Harris, 1997)

$$f_{c1} = \frac{\int_0^{\infty} f |A_1(f)| df}{\int_0^{\infty} |A_1(f)| df}, \quad (19)$$

and the variance can be given as

$$\sigma_1^2 = \frac{\int_0^{\infty} (f - f_{c1})^2 |A_1(f)| df}{\int_0^{\infty} |A_1(f)| df}. \quad (20)$$

Similarly, for the amplitude spectrum of output signal, its' centroid frequency and variance are defined as

$$f_{c2} = \frac{\int_0^{\infty} f |A_2(f)| df}{\int_0^{\infty} |A_2(f)| df} \quad (21)$$

and

$$\sigma_2^2 = \frac{\int_0^\infty (f-f_{c2})^2 |A_2(f)| df}{\int_0^\infty |A_2(f)| df}. \quad (22)$$

Due to preferential attenuation of high frequency component, there is a downshift of centroid frequency. This centroid frequency-shift is connected to the Q attenuation as (Quan and Harris, 1997)

$$\int_{ray} \frac{\pi}{Qv} dl = \frac{f_{c1}-f_{c2}}{\sigma_1^2}. \quad (23).$$

The left-hand side of equation (23) can be formulated as

$$\int_{ray} \frac{\pi}{Qv} dl = \frac{\pi\tau}{Q_{int}}, \quad (24)$$

where Q_{int} is the interval/average Q corresponding to the interval travel time τ for this attenuation process. Then, Q can be estimated as

$$Q_{est} = \frac{\pi\tau\sigma_1^2}{f_{c1}-f_{c2}}. \quad (25)$$

Quan and Harris (1997) derive equation (23) with assumption that $|A_1(f)|$ is of Gaussian shape. In practice, this assumption might not be perfectly meet and the spectrum can be approximately regarded as Gaussian.

As shown in equation (25), the final estimated Q value is proportional to calculated centroid frequency-shift ($f_{c1} - f_{c2}$) and variance σ_1^2 . The fluctuations of the high frequency components of $|A_1(f)|$ and $|A_2(f)|$ may bring perturbation to the calculation of f_{c1} , f_{c2} and σ_1^2 , which can significantly affect the estimation result. With the assumption that the amplitude spectrum is Gaussian, the centroid frequency of power spectrum will remain unchanged, and the variance of the power spectrum, calculated according to equation (22) will be half of the variance calculated from amplitude spectrum. To stabilize the estimation result, a second approach can be that f_{c1} , f_{c2} are estimated from the corresponding power spectra and the variances are estimated from amplitude spectra. The third approach can be that both the centroid frequency and variance can be estimated from power spectra. In addition, a limited frequency band instead of the whole frequency range can be used to calculate the centroid frequencies and variances.

Match-filter method

Cheng and Margrave (2012) propose a match-filter method for Q estimation. The procedure of this method consists of three stages. First the smoothed amplitude spectra $|A_1(f)|$ and $|A_2(f)|$ are estimated for the two local wavelets by a multitaper method introduced by Thomsen (1985). Then, the minimum-phase wavelets $w_1(t)$ and $w_2(t)$ with amplitude spectra $|A_1(f)|$ and $|A_2(f)|$ respectively are computed. Finally, Q can be estimated by

$$Q_{\text{est}} = \min_Q \|w_1(t) * I(Q, t) - \mu w_2(t)\|^2, \quad (26)$$

where * denotes convolution, and $I(Q, t)$ is the impulse-response of the constant-Q theory with a quality factor value Q and travel time $(t_2 - t_1)$, which can be formulated as

$$I(Q, t) = F^{-1}\left(\exp\left(\frac{-\pi f(t_2-t_1)}{Q} - iH\left(\frac{\pi f(t_2-t_1)}{Q}\right)\right)\right), \quad (27)$$

μ is a constant scaling factor which accounts for frequency independent loss and can be estimated as

$$\mu = \frac{\int_{-\infty}^{\infty} (w_1(t) * I(Q, t)) w_2(t) dt}{\int_{-\infty}^{\infty} w_2^2(t) dt}. \quad (28)$$

For the match-filter method described by equation (26), the optimal Q is found by a direct search over an assumed range of Q values with a particular increment since it is a nonlinear minimization.

The complex spectral-ratio method and centroid frequency-shift method are frequency-domain methods. Both of them may need to define a frequency range where signal dominates for better estimation. The match-filter method is a time-domain. In practical application, bandpass filters are usually applied to local wavelets to obtain better estimation of minimum-phase equivalent wavelets. In this paper, the performance of these three methods will be evaluated by synthetic data and real VSP data.

NUMERICAL TEST

Synthetic 1D VSP data or reflection data with isolated reflectors

First, we use synthetic noise free VSP data to validate the Q estimation methods theoretically. A synthetic attenuated seismic trace was created by a nonstationary convolution model proposed by Margrave (1998), using two isolated reflectors, a minimum phase wavelet with dominant frequency of 40 Hz and a constant Q value of 80, as shown in figure 1. Using the two local events in figure 1, Q estimations from the three methods are conducted. For the complex spectral ratio method, the exact reference frequency is used to construct vector M_2 formulated in equation (10) at this time. The complex spectral-ratio method reduces to the classic spectral-ratio method when only amplitude spectra are employed for Q estimation and gives exact estimation, as shown in figure 2. Figure 3 shows the estimation result of $Q = 79.55$ when only phase spectra are employed. For the centroid frequency method, we use the entire frequency band to compute the centroid frequencies and variance at this time, and we refer the case that both centroid frequencies and variance are estimated from amplitude spectrum as approach 1, the case that frequencies are calculated from power spectra while variances are calculated from amplitude spectra as approach 2, and the case that both centroid frequencies and variances are calculated from power spectra as approach 3. The estimation result of $Q = 114.82$ for approach 1 is biased since the amplitude spectra deviate from Gaussian, as shown in figure 4. For approach 2, the estimation result is $Q = 197.65$. At this occasion, the downshift of centroid frequency is smaller since the power spectra have condensed curves compared to the original amplitude spectra, as shown in figure 5. According to equation (25), smaller frequency shift leads to larger

estimated Q value. For approach 3, the estimated Q is 100.7. The employment of power spectrum suppresses the high frequency components for the calculation of centroid frequencies and variances, and lead to a more close estimation, as shown in figure 6. For the match-filter method, it gives an estimation of 80.06 when fitting error is minimized, as shown in figure 7 and figure 8.

For the centroid frequency-shift method, when the original amplitude spectra of signals are obviously different from Gaussian, using the whole frequency band to calculate centroid frequencies and variances give biased results, which lead to deviated Q estimation. Figure 9 shows the case of approach 1 with frequency bands of $5\text{Hz} - 120\text{Hz}$ and $5\text{Hz} - 90\text{Hz}$ for the two local wavelets respectively, and the Q estimation result is $Q = 76.11$. Figure 10 shows the case of approach 2 with frequency bands of $5\text{Hz} - 100\text{Hz}$ and $5\text{Hz} - 80\text{Hz}$ for the two local wavelets respectively, and the Q estimation result is $Q = 82.03$. Figure 11 shows that case of approach 3 with frequency bands of $5\text{Hz} - 80\text{Hz}$ and $5\text{Hz} - 60\text{Hz}$ for the two local wavelets respectively, and the estimation result is $Q = 75.39$. With appropriately chosen frequency band, better estimation of the centroid frequencies and variances are obtained, and the estimation result is improved.

Then, random noise is added to the synthetic data to evaluate the performance of the Q -estimation methods in more practical circumstances. Figure 12 shows a synthetic seismic trace with a signal-to-noise ratio of $SNR = 4$ (we define this in the time domain as the ration of the RMS values of signal and noise). The amplitude spectra of the two events are show in Figure 13 and Figure 14, of which the noise levels are about -25DB and -20DB respectively. The two local events in Figure 12 are used to test the three Q -estimation methods discussed in this paper. For the complex spectral-ratio method, a frequency range of $15\text{Hz} - 75\text{Hz}$ is used for Q estimation. For the centroid frequency-shift method, the same frequency bands as the noise free case tested above are chosen for the three approaches. For the match-filter method, band-pass filters are applied to suppress the noise before estimating the embedded wavelets, and the passing bands for the two local wavelets are $10\text{Hz} - 140\text{Hz}$ and $10\text{Hz} - 90\text{Hz}$ respectively. The smoothing of amplitude spectra using multitaper method is not conducted for the math-filter method. To make a more general comparison of performance for the estimation methods in presence of noise, 200 seismic traces are created by adding 200 different random noise series of the same level ($SNR = 4$) to the trace shown in Figure 12. Then Q estimation is conducted using these noise contaminated data. The histograms of the estimated Q values are shown in Figure 15 - 21. For the complex spectral-ratio method, it reduces to the classic spectral-ratio method when only amplitude spectra are employed, the estimation results have a mean value of 87.08 and standard deviation of 26.74, as shown in Figure 15. When only the phase spectra are used for Q estimation, the results have a mean value of 80.32 and standard deviation of 7.13, as shown in Figure 16. When both amplitude spectra and phase spectra are used for Q estimation, Figure 17 shows the results based on equation (18) with $\varepsilon = 0.5$. We can see that the employment of phase information significantly improve the estimation results for the complex spectral-ratio method. For the centroid frequency-shift method, the estimation results for the three approach are comparable, as shown in Figure 18 - 20. For the match-filter method, the estimation results has a mean value of 80.79 and standard deviation of 7.07, as shown in

Figure 21. Overall, the estimation results for all these methods are comparable, while the results of complex spectral-ratio method and match-filter method are slightly better.

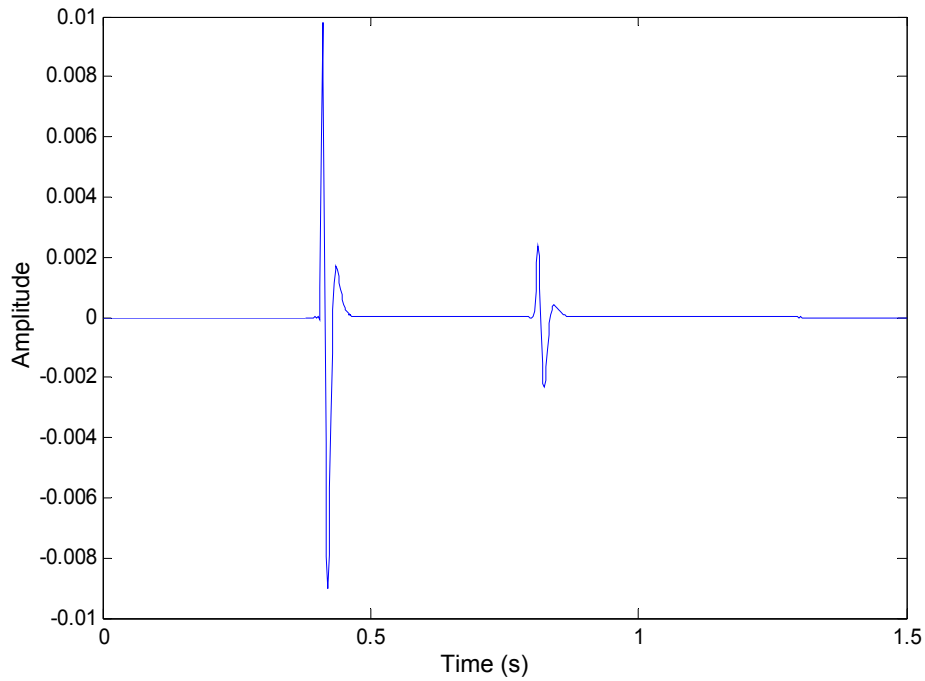


Figure 1. Synthetic seismic trace created with two events, created using two isolated reflectors, a minimum phase source wavelet with dominant frequency of 40Hz, and a constant Q value of 80.

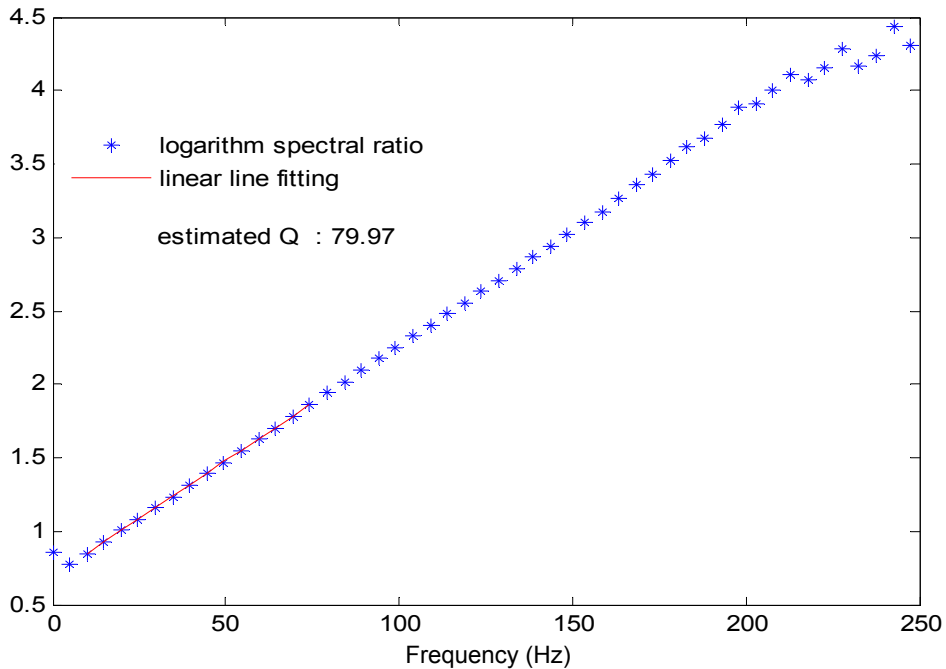


Figure 2. Q estimation by complex spectral-ratio method using the two local events shown in figure 1.

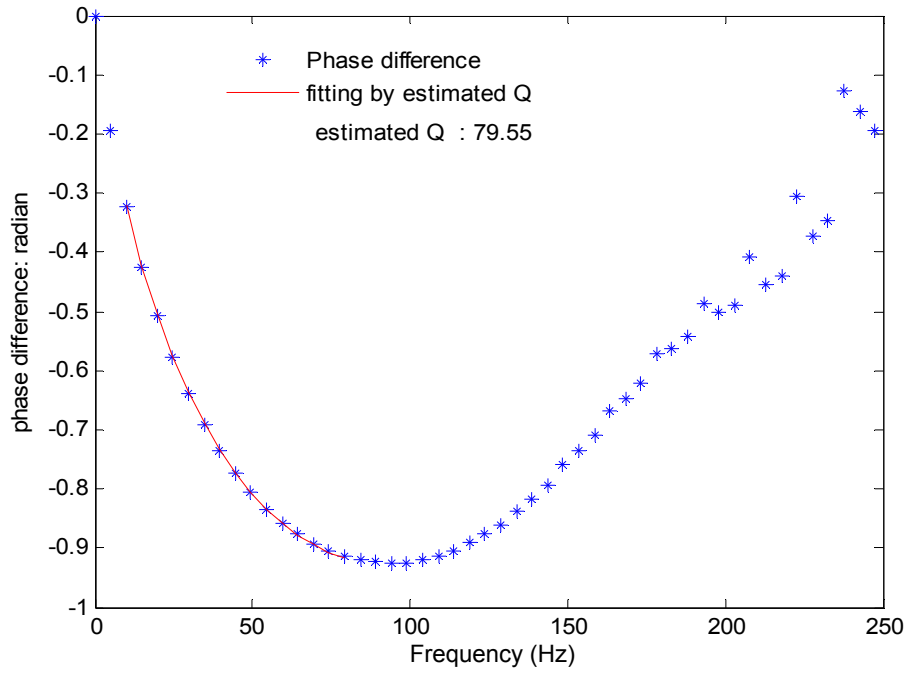


Figure 3. Q estimation by the complex spectral-ratio method using the two local events shown in Figure 1 when only phase spectra are employed.

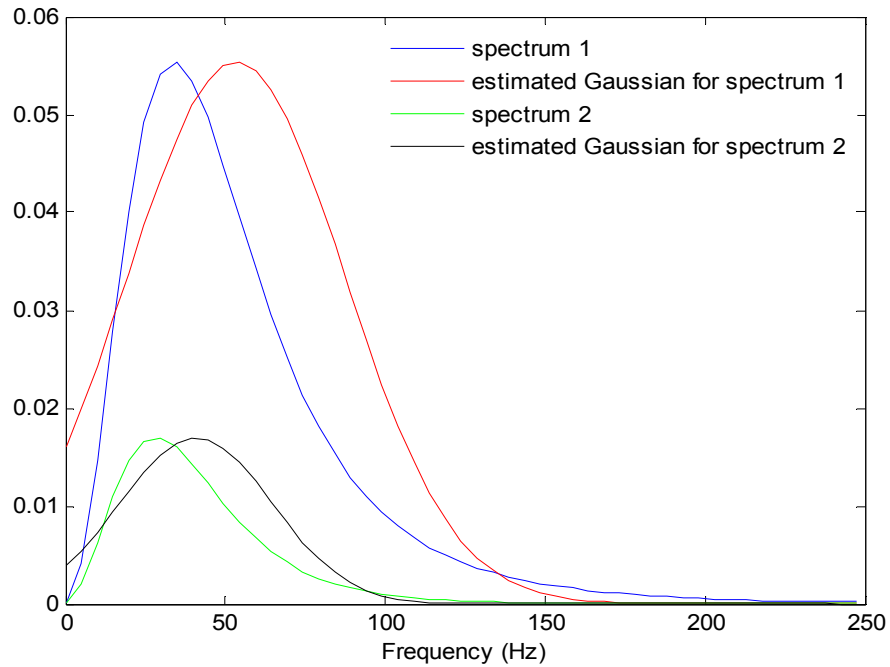


Figure 4. Q estimation by the centroid frequency-shift method using the two local events shown in Figure 1.

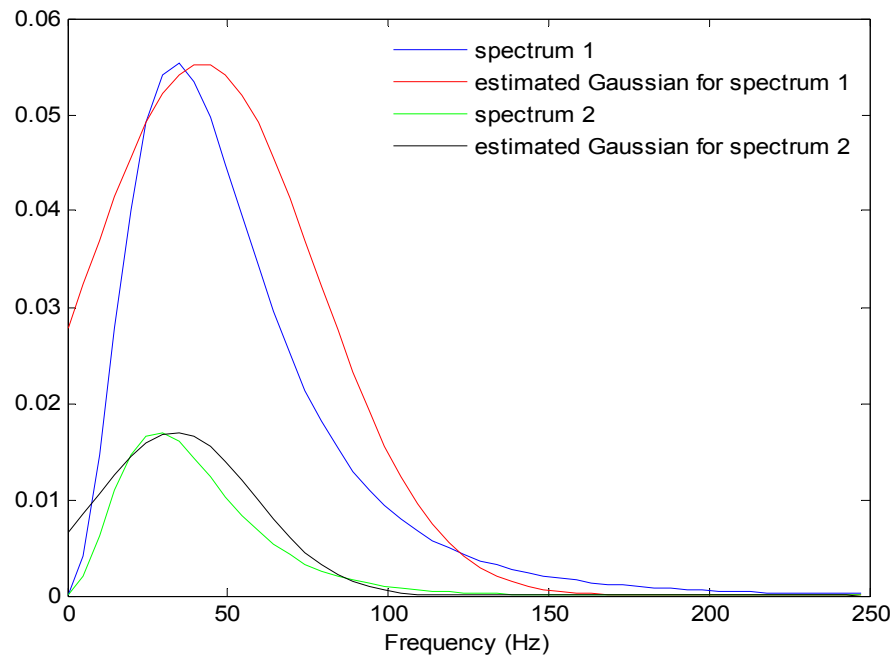


Figure 5. Q estimation by the centroid frequency-shift method using the two local events shown in Figure 1 (centroid frequencies are estimated from power spectrum).

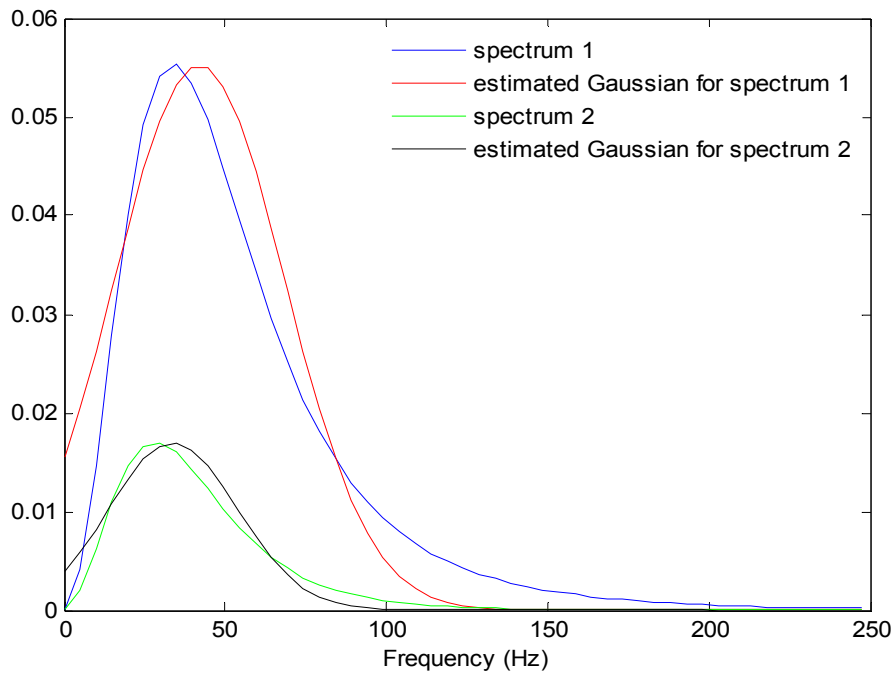


Figure 6. Q estimation by the centroid frequency-shift method using the two local events shown in Figure 1 (both centroid frequencies and variance are estimated from power spectrum).

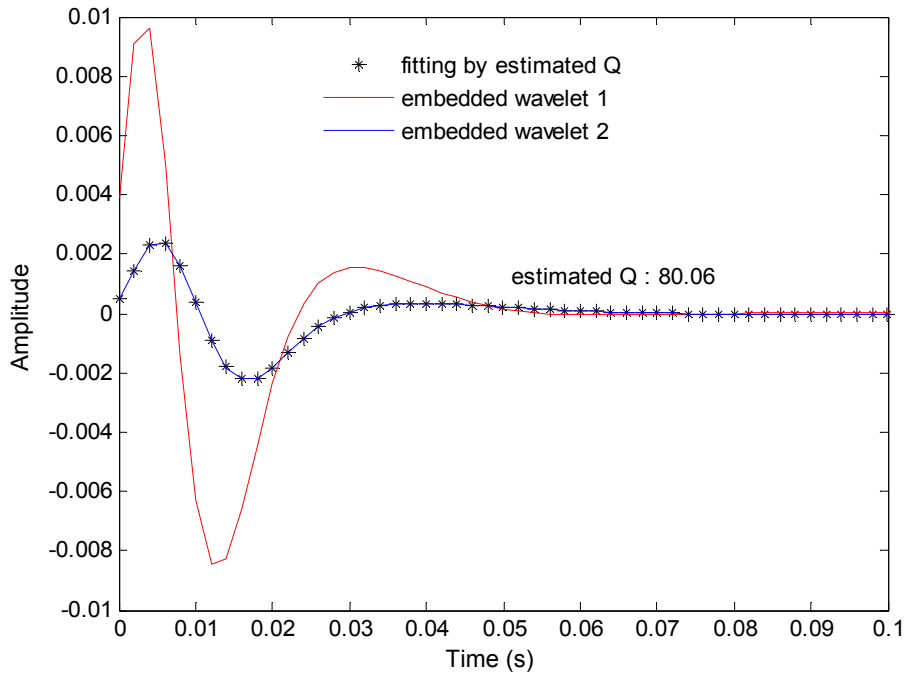


Figure 7. Q estimation by the match-filter method using the two local events shown in figure 1.

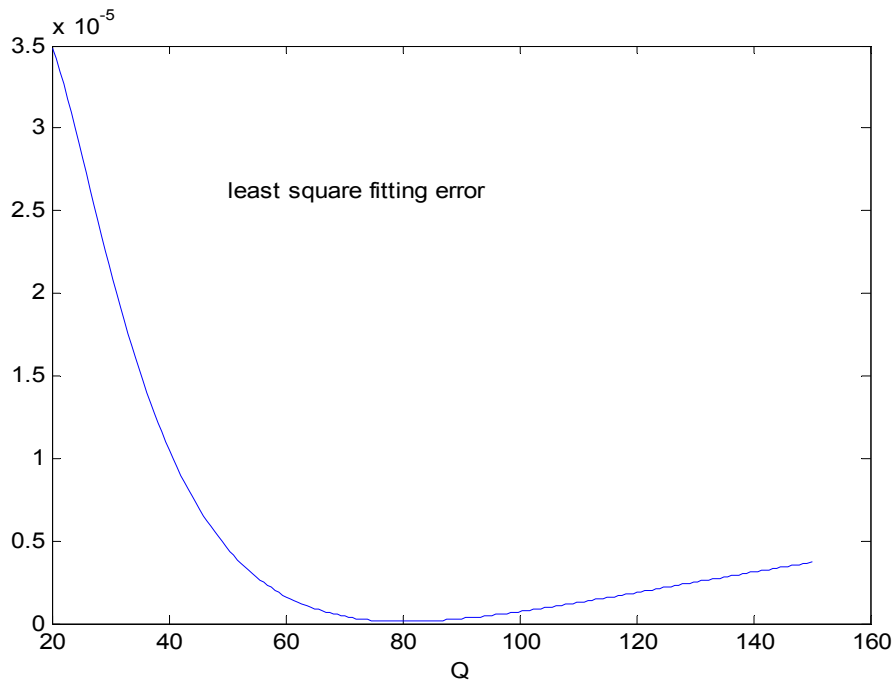


Figure 8. The fitting error curve for Q estimation by match-filter method corresponding to figure 7.

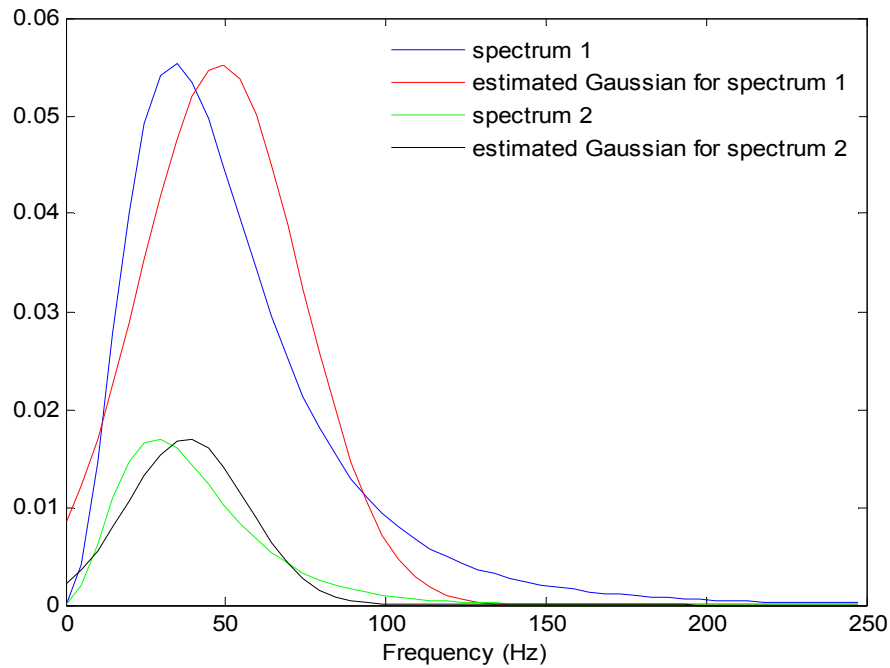


Figure 6. Q estimation by the centroid frequency-shift method using the two local events shown in Figure 1. Both centroid frequencies and variance are estimated from the amplitude spectra of the local wavelets with frequency band of 5Hz – 120Hz and 5Hz – 90Hz respectively.

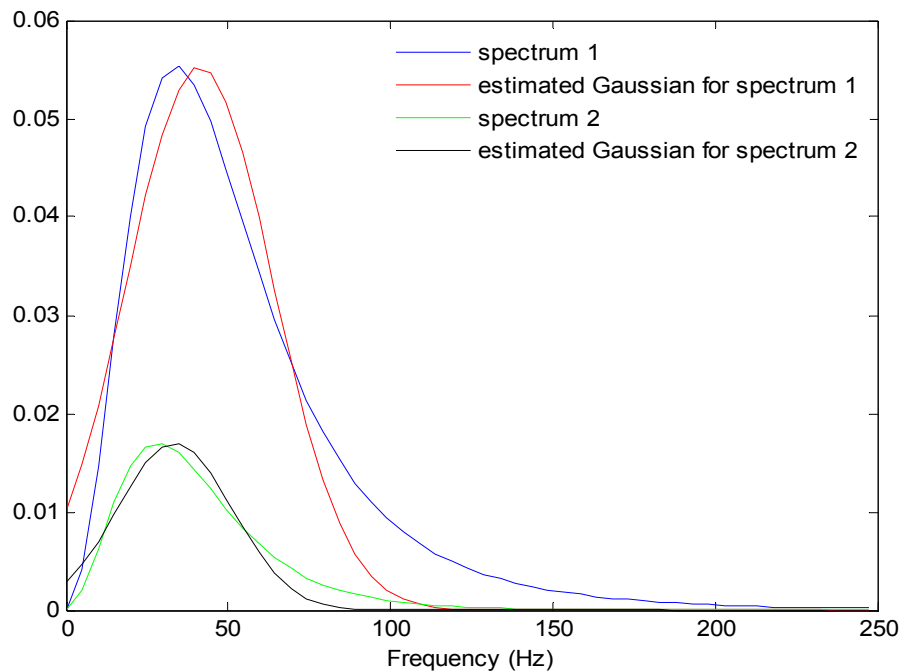


Figure 10. Q estimation by the centroid frequency-shift method using the two local events shown in Figure 1. The centroid frequencies and variance are estimated from the power spectra of the local wavelets while the variances are calculated from amplitude spectra with frequency band of 5Hz – 120Hz and 5Hz – 90Hz respectively.

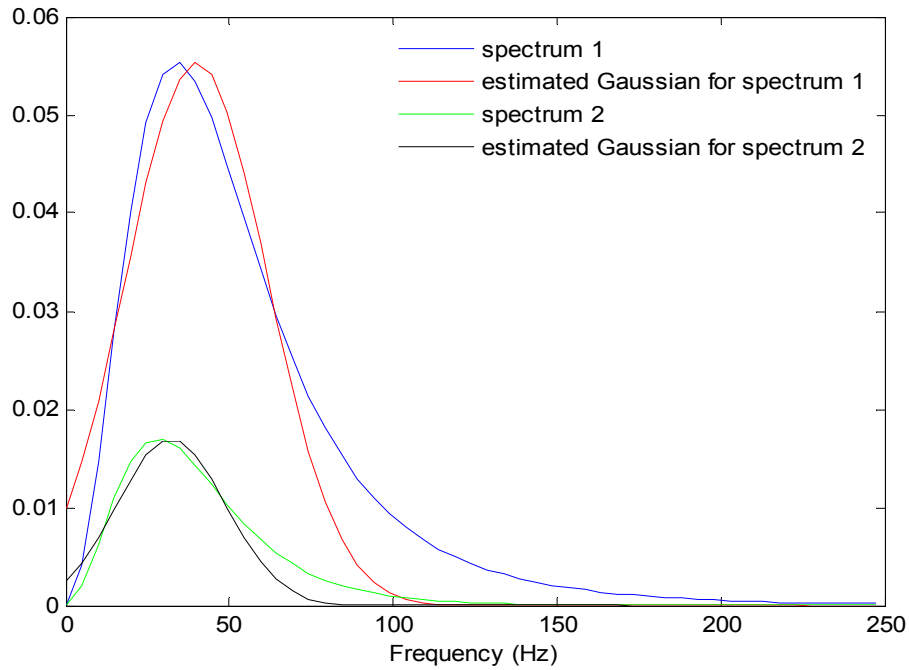


Figure 11. Q estimation by the centroid frequency-shift method using the two local events shown in Figure 1. Both centroid frequencies and variance are estimated from the power spectra of the local wavelets with frequency band of 5Hz – 80Hz and 5Hz – 60Hz respectively

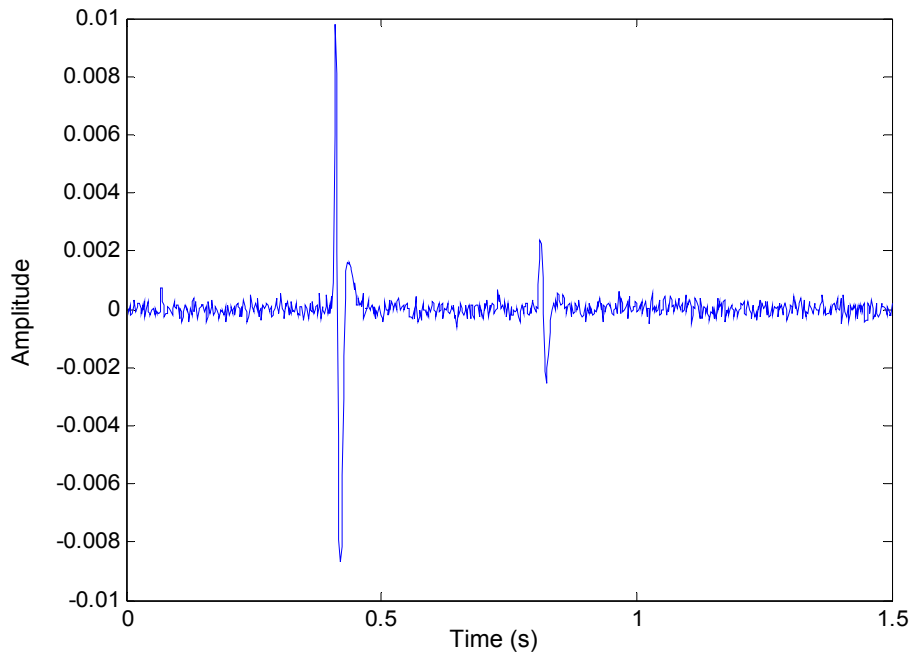


Figure 12. Synthetic seismic trace with noise, created by adding random noise to the seismic trace in Figure 3.1 with SNR=4. Local event 1 at 0.34s-0.54s and event 2 at 0.74s-0.94s are picked for Q estimation tests.

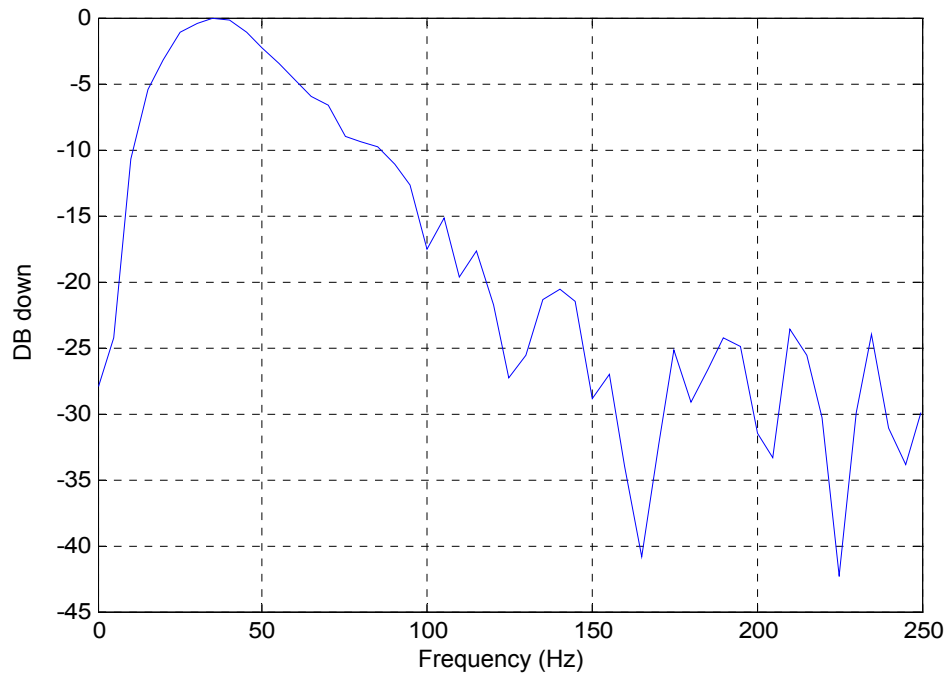


Figure 13. Amplitude spectrum of the local event 1 (0.34s-0.54s) in Figure 12.

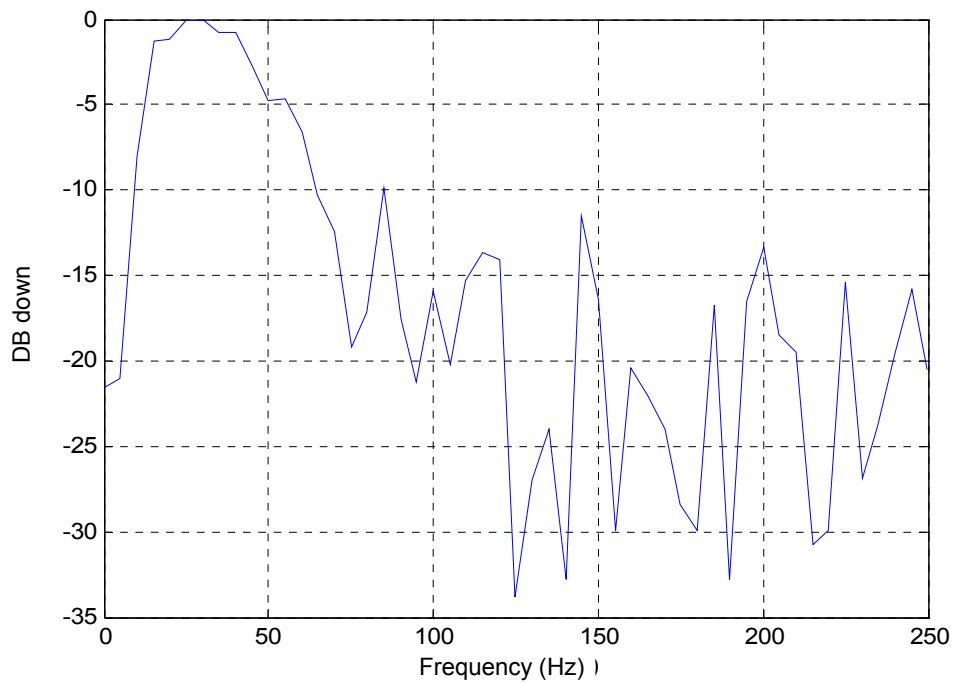


Figure 14. Amplitude spectrum of the event 2 (0.74s-0.94s) second in Figure 12.

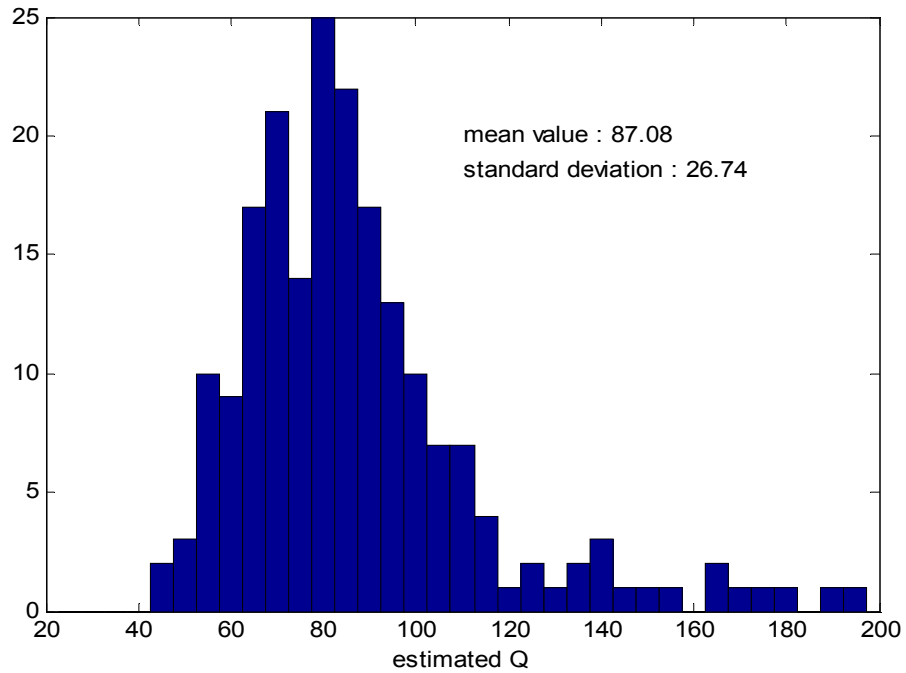


Figure 15. Histogram of the Q values estimated by complex spectral-ratio method (only amplitude spectra are employed) using 200 seismic traces (similar to the one shown in Figure 12) with noise level of $SNR = 4$.

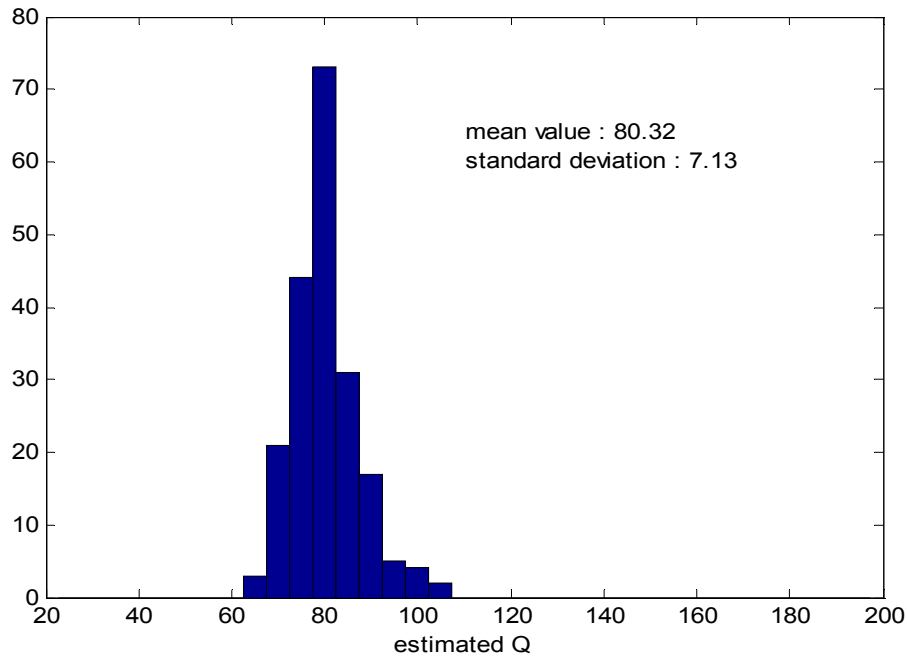


Figure 16. Histogram of the Q values estimated by complex spectral-ratio method (only phase spectra are employed) using 200 seismic traces (similar to the one shown in Figure 12) with noise level of $SNR = 4$.

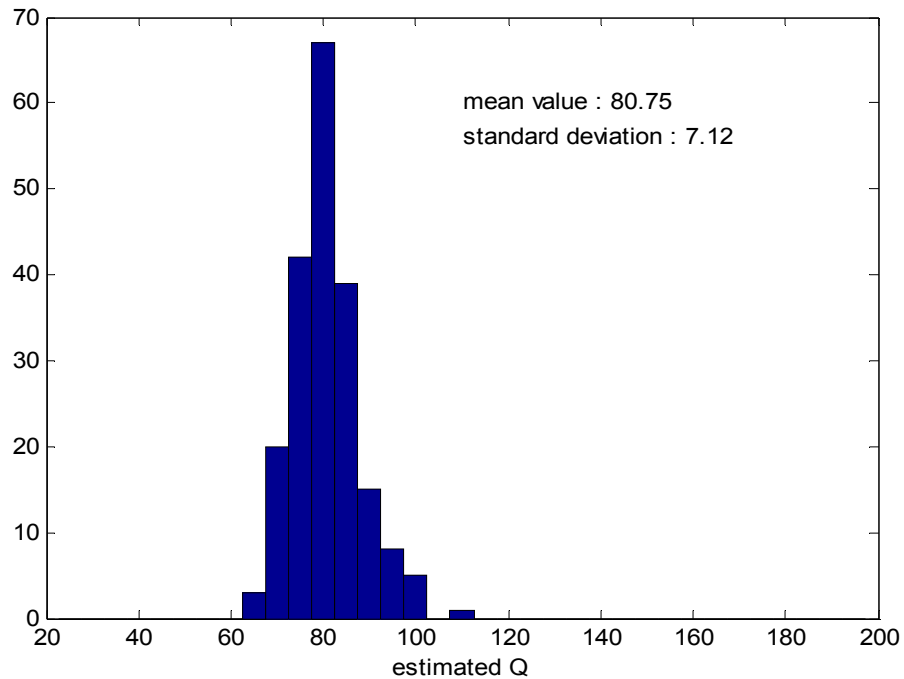


Figure 17. Histogram of the Q values estimated by generalized complex spectral-ratio method based on equation (18) with $\varepsilon = 0.5$, using 200 seismic traces (similar to the one shown in Figure 12) with noise level of $SNR = 4$.

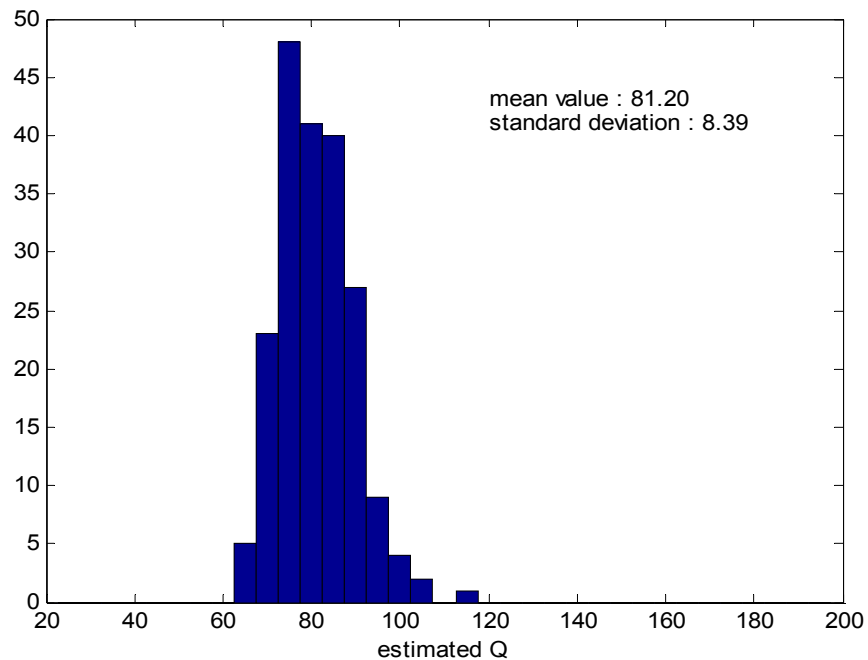


Figure 18. Histogram of the Q values estimated by centroid frequency-shift method using 200 seismic traces (similar to the one shown in Figure 12) with noise level of $SNR = 4$. Both centroid frequencies and variance are estimated from the amplitude spectra of the local wavelets with frequency band of 5Hz – 120Hz and 5Hz – 90Hz respectively.

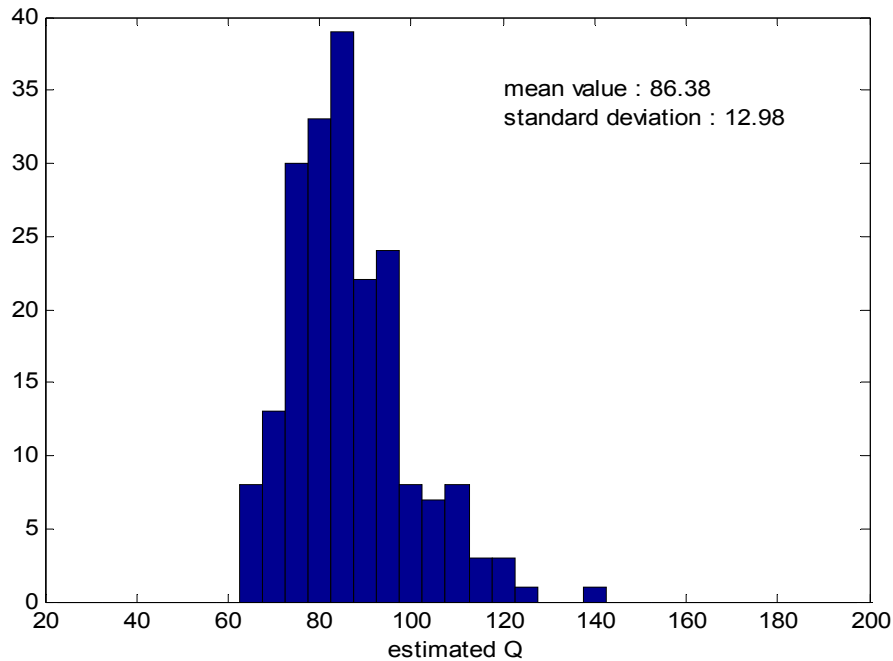


Figure 19. Histogram of the Q values estimated by centroid frequency-shift method using 200 seismic traces (similar to the one shown in Figure 12) with noise level of $SNR = 4$. Both centroid frequencies are estimated from power spectrum and variances are estimated from the amplitude spectra of the local wavelets with frequency band of 5Hz – 100Hz and 5Hz – 80Hz respectively.

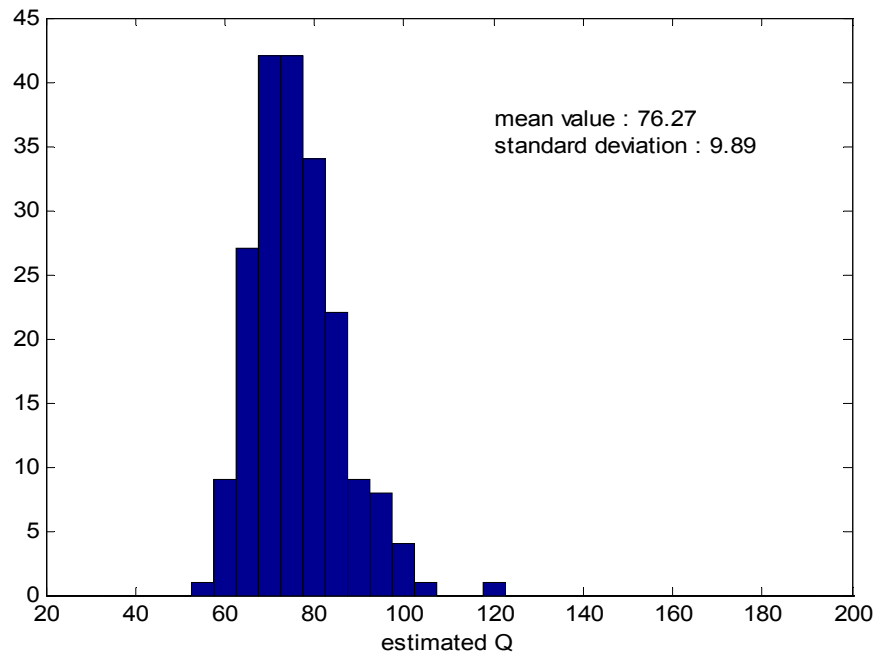


Figure 20. Histogram of the Q values estimated by centroid frequency-shift method using 200 seismic traces (similar to the one shown in Figure 12) with noise level of $SNR = 4$. Both centroid frequencies and variance are estimated from the power spectra of the local wavelets with frequency bands of 5Hz – 80Hz and 5Hz – 60Hz respectively.

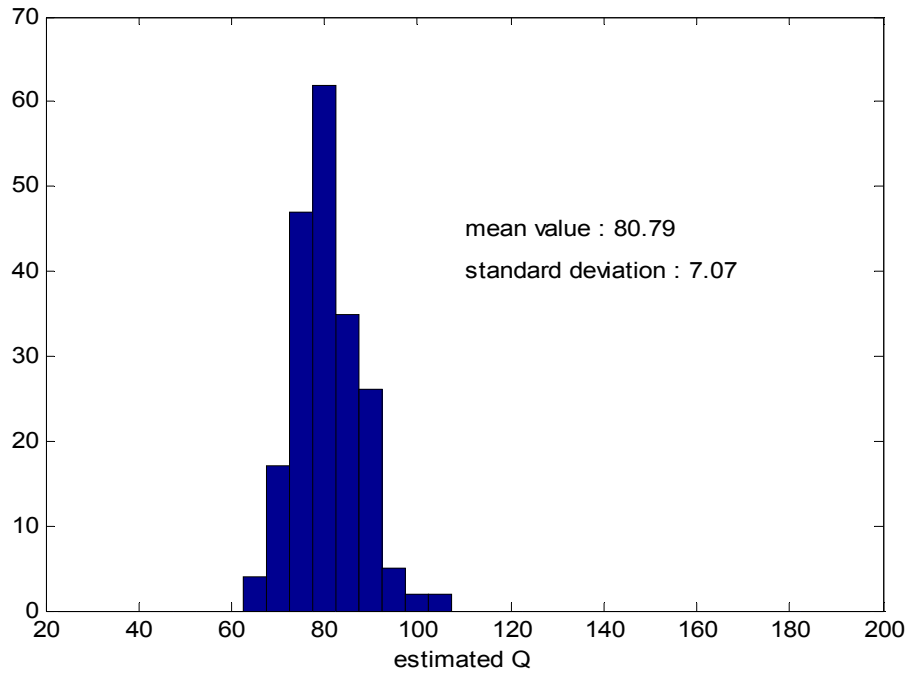


Figure 21. Histogram of the Q values estimated by the match-filter method using 200 seismic traces with noise level of $SNR = 4$ (multitaper method is employed for spectrum estimation).

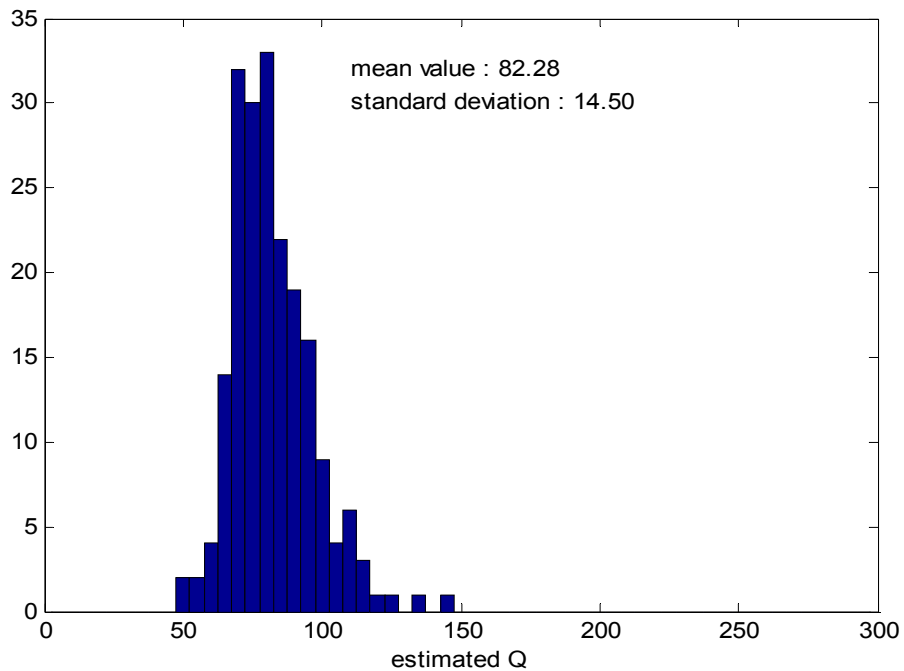


Figure 22 Histogram of the Q values estimated by complex spectral-ratio method (only phase spectra are employed) using 200 seismic traces (similar to the one shown in Figure 12) with noise level of $SNR = 2$.

In addition, synthetic VSP data with extensive noise are used to evaluate Q estimation methods. The Q estimation is conducted using 200 seismic traces with noise level of $SNR = 2$. For the complex spectral ratio method, Q estimation is conducted for two cases. The first case is that only the phase spectra are used for Q estimation; the second case is the generalized complex spectral-ratio method based on equation (18) with $\varepsilon = 0.5$. As shown in Figure 22 – 23, the results of these two cases are comparable. It might indicate that the phase difference between the local wavelets is not significantly affected by the increased noise level. For the centroid frequency-shift method, the estimation results are shown in Figure 24 – 26 for the three approaches when spectrum smoothing is not employed. We can see that the estimation result is affected by the increased noise level and have deviated mean values and larger standard deviation values. When the spectrum smoothing by multitaper method is incorporated for these three approaches, the corresponding estimation result are improved, as shown in Figure 27 – 29. The match-filter method, as shown in Figure 30, still gives quite good estimation with a mean value of 80.02 and standard deviation of 11.82, which is slightly better than the results of complex spectral ratio method and centroid frequency-shift method. Based on the above results, we can see that all the three methods are comparable and robust to noise.

For the complex spectral-ratio method, its' estimation result is subject to the choosing of reference frequency. The accurate reference frequency f_0 (the Nyquist frequency) is used for the above tests. To evaluate the influence of inaccurate reference frequency for the complex spectral-ratio method, only the phase spectra are used to give estimation result and f_0 is chosen as the Nyquist frequency scaled by 0.8. First, Q estimation is conducted using the two local events shown in Figure 1. As shown in Figure 31, the estimated Q of 68.32 is deviated from true value 80 for this ideal case. Then, Q estimation is conducted using 200 seismic traces, similar to the one shown in Figure 12, with noise level of $SNR = 4$ and $SNR = 2$ respectively. The distributions of corresponding estimated Q values are shown in Figure 32 and 33. We can see that the mean value of the estimation results is consistent with the ideal case shown in Figure 31, which is deviated from true value, and the standard deviation values of the estimated results remain at the same level as the cases with accurate reference frequency shown in Figure 16 and 22. Therefore, the complex spectral-ratio method is robust to noise, however its accuracy will depend on how well the reference frequency is chosen to match the data.

For the centroid frequency-shift method, the estimation result is subject to the frequency bands chosen to calculate the centroid frequencies and variances for the local wavelets. The chosen frequency bands can significantly since the final estimation result. It is not trivial to choose appropriately frequency bands for both frequency bands since they are not chosen based on SNR or dominant frequency band. We choose the frequency bands that give good estimation results based on testing with different choices. Theoretically, the frequency bands used to filter the local wavelets for noise suppression can affect the result of match-filter method as well. The frequency bands for the Q estimation tests shown above are chosen based on the SNR level.

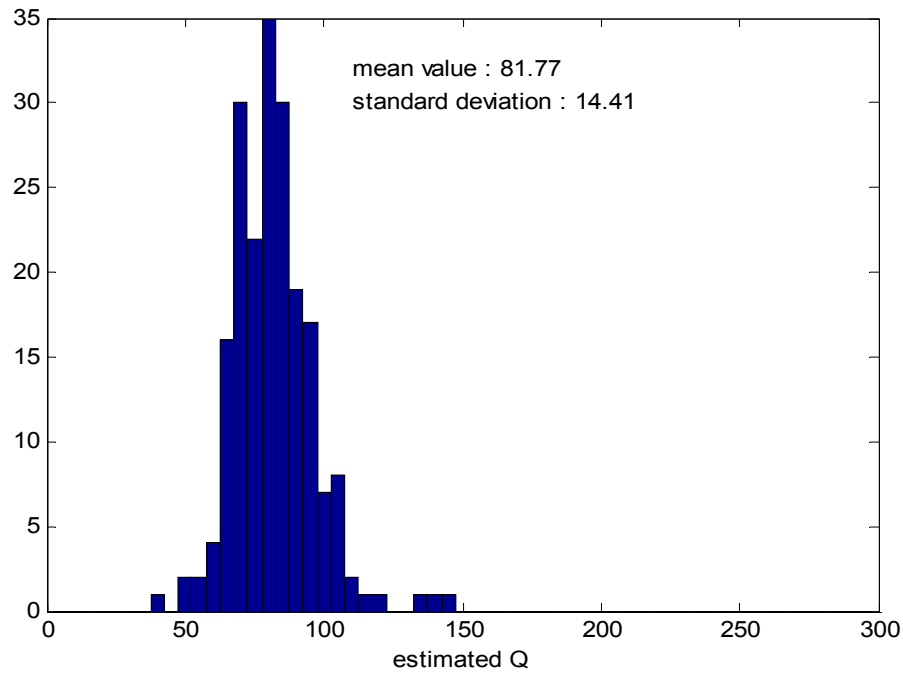


Figure 23. Histogram of the Q values estimated by generalized complex spectral-ratio method based on equation (18) using 200 seismic traces (similar to the one shown in Figure 12) with noise level of $SNR = 2$.

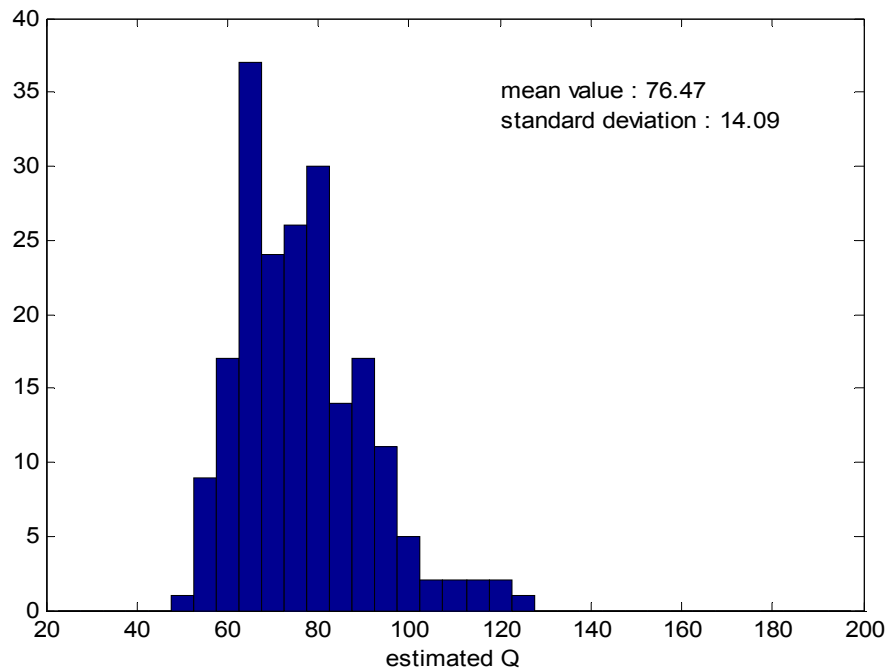


Figure 24. Histogram of the Q values estimated by centroid frequency-shift method using 200 seismic traces (similar to the one shown in Figure 12) with noise level of $SNR = 2$. Both centroid frequencies and variance are estimated from the amplitude spectra of the local wavelets with frequency band of 5Hz – 110Hz and 5Hz – 80Hz respectively.

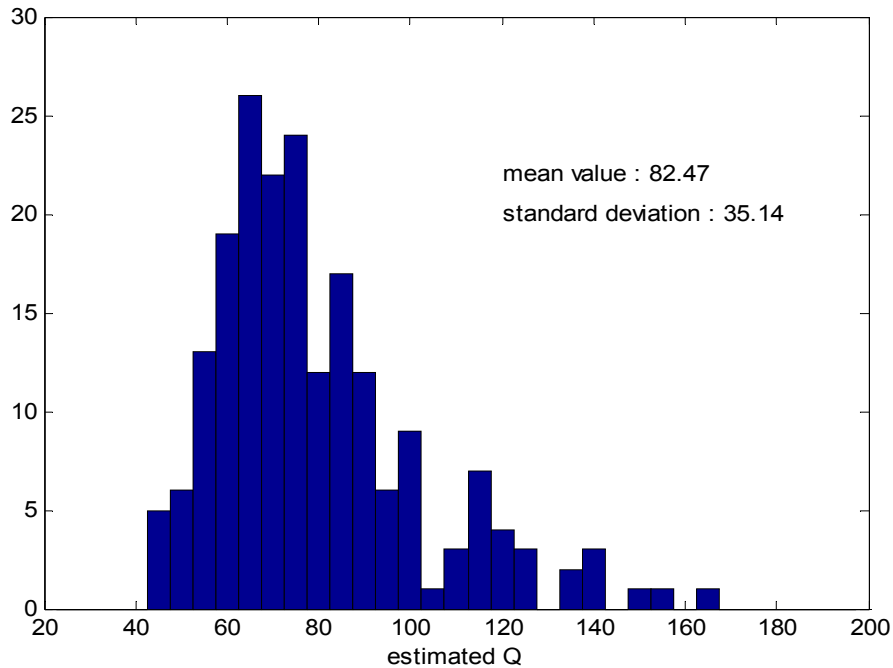


Figure 25. Histogram of the Q values estimated by centroid frequency-shift method using 200 seismic traces (similar to the one shown in Figure 12) with noise level of $SNR = 2$. Both centroid frequencies are estimated from power spectrum and variances are estimated from the amplitude spectra of the local wavelets with frequency band of 5Hz – 90Hz and 5Hz – 70Hz respectively.

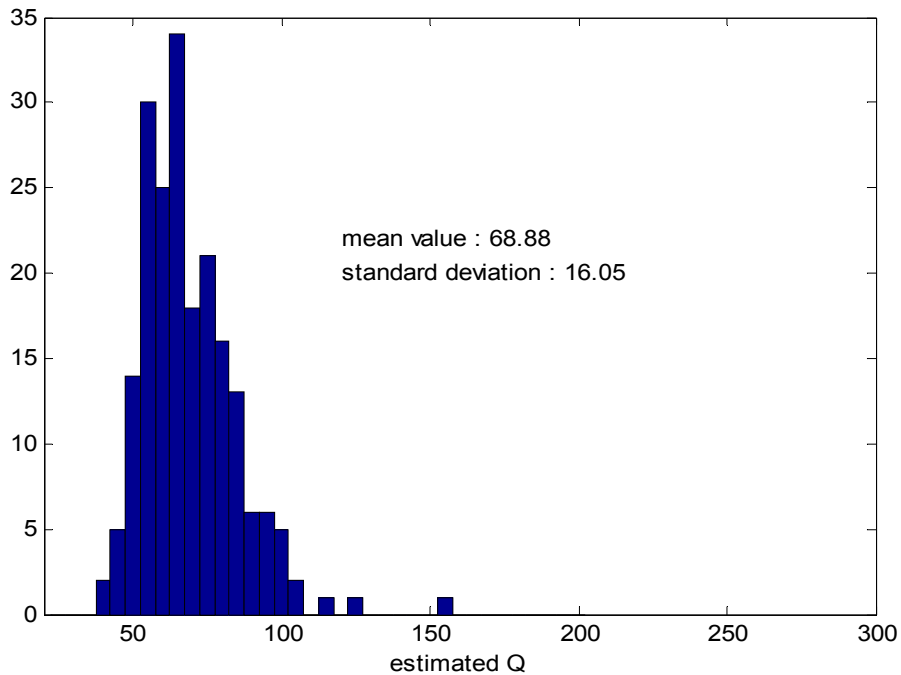


Figure 26. Histogram of the Q values estimated by centroid frequency-shift method using 200 seismic traces (similar to the one shown in Figure 12) with noise level of $SNR = 4$. Both centroid frequencies and variance are estimated from the power spectra of the local wavelets with frequency bands of 5Hz – 75Hz and 5Hz – 55Hz respectively.

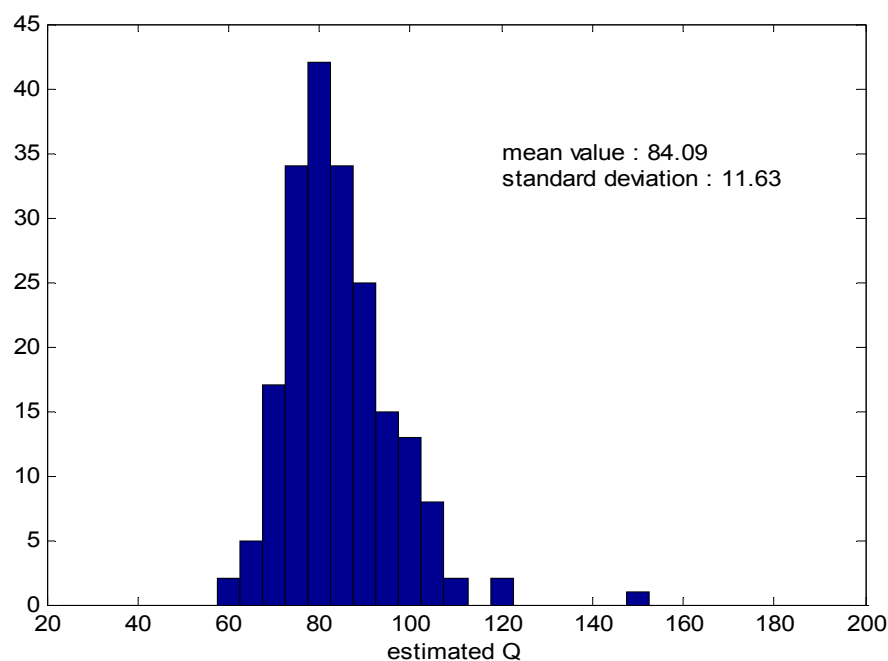


Figure 27. Histogram of the Q values estimated by centroid frequency-shift method using 200 seismic traces (similar to the one shown in Figure 12) with noise level of $SNR = 2$. Both centroid frequencies and variance are estimated from the amplitude spectra of the local wavelets with frequency band of 5Hz – 110Hz and 5Hz – 80Hz respectively (the multitaper method is incorporated for spectrum smoothing).

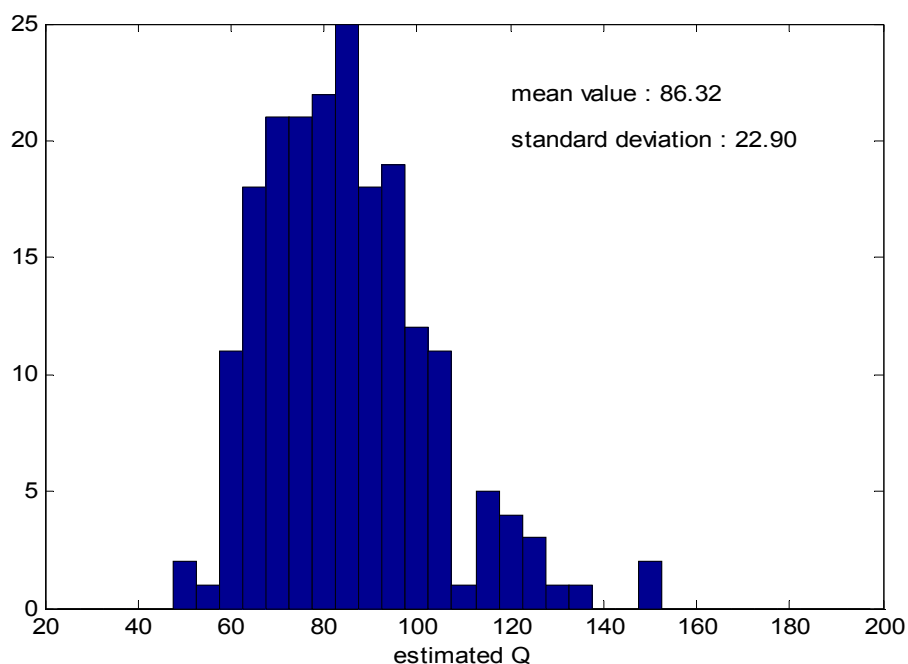


Figure 28. Histogram of the Q values estimated by centroid frequency-shift method using 200 seismic traces (similar to the one shown in Figure 12) with noise level of $SNR = 2$. Both centroid frequencies are estimated from power spectrum and variances are estimated from the amplitude spectra of the local wavelets with frequency band of 5Hz – 90Hz and 5Hz – 70Hz respectively (the multitaper method is incorporated for spectrum smoothing).

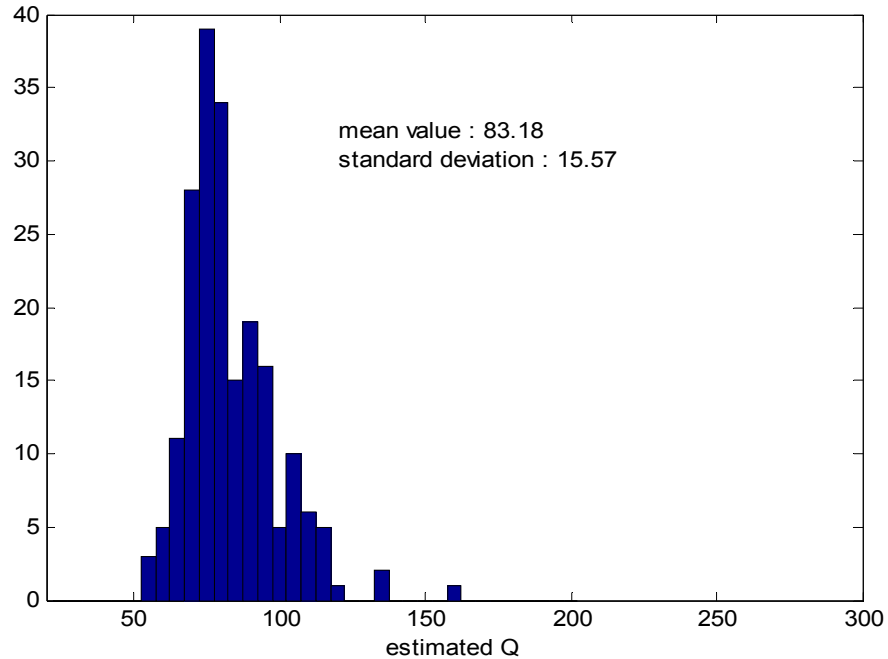


Figure 29. Histogram of the Q values estimated by centroid frequency-shift method using 200 seismic traces (similar to the one shown in Figure 12) with noise level of $SNR = 4$. Both centroid frequencies and variance are estimated from the power spectra of the local wavelets with frequency bands of 5Hz – 75Hz and 5Hz – 55Hz respectively (the multitaper method is incorporated for spectrum smoothing).

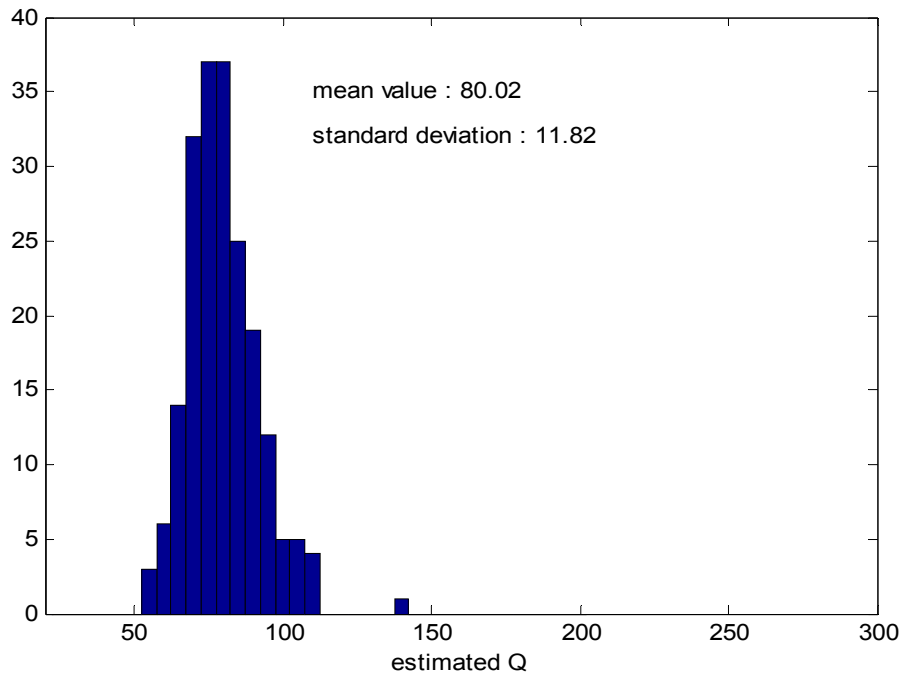


Figure 30. Histogram of the values estimated by the match-filter method using 200 seismic trace (similar to the one shown in Figure 12) with noise level of $SNR=2$ (multitaper method is employed for spectrum estimation).

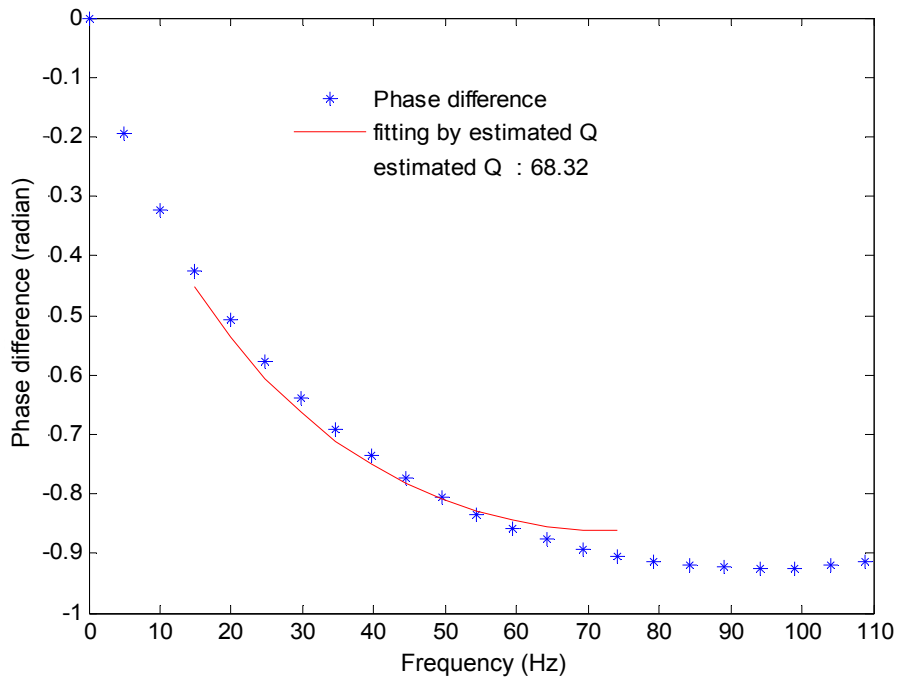


Figure 31. Q estimation by complex spectral-ratio method (only phase spectra are employed) using the two events shown in Figure 1 (inaccurate reference frequency is used).

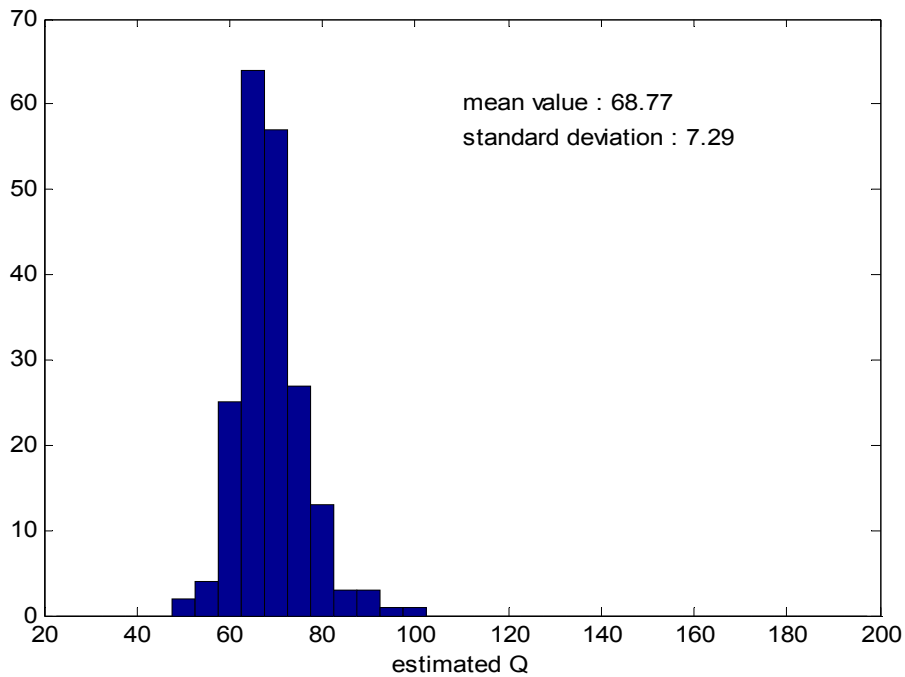


Figure 32. Histogram of the Q values estimated by complex spectral-ratio method (only phase spectra are employed) using 200 seismic traces (similar to the one shown in Figure 12) with noise level of $SNR = 2$ (inaccurate reference frequency is used).

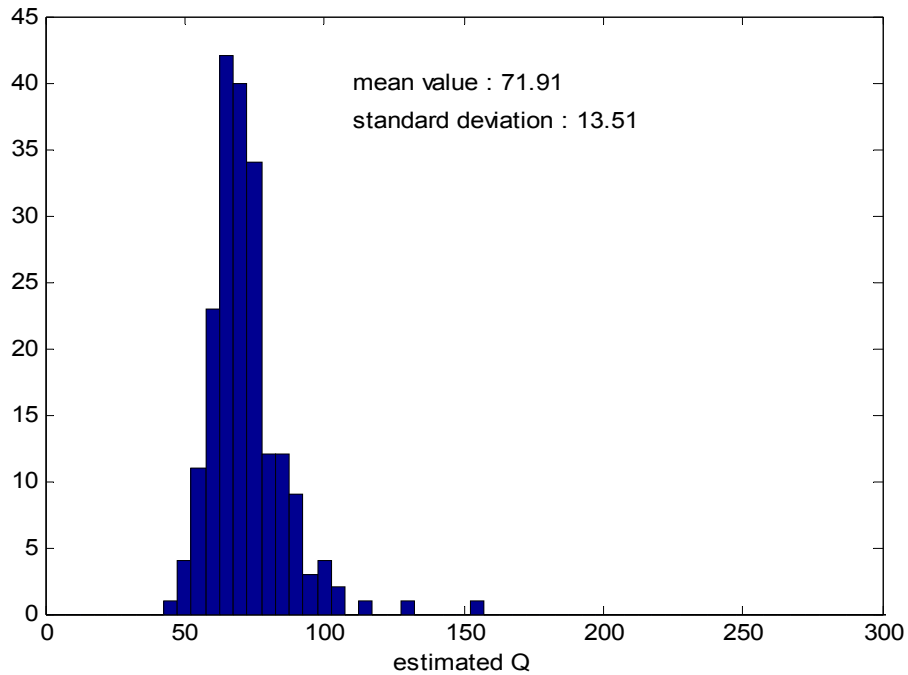


Figure 33. Histogram of the Q values estimated by complex spectral-ratio method (only phase spectra are employed) using 200 seismic traces (similar to the one shown in Figure 12) with noise level of $SNR = 2$ (inaccurate reference frequency is used).

Synthetic 1D reflection data

Surface reflection data is the most common seismic data. We use the synthetic reflection data to evaluate the centroid frequency-shift method and the match-filter method. For the centroid frequency shift method, only the approach with centroid frequencies and variances calculated from amplitude spectra will be tested, since all the three approaches can obtain similar results. A synthetic seismic trace is created using a random reflectivity series, a minimum phase source wavelet with dominant frequency of 40Hz and a constant Q of 80, as shown in Figure 34. Two local reflected waves are obtained by applying time gates of 100ms – 500ms and 900ms – 1300ms to the attenuated seismic trace. For the two windowed local waves, their spectrum estimation by multitaper method is demonstrated by Figure 35. The spikes and notches in the original spectra of local reflected waves are obvious, which are caused by the tuning effect of local reflectors. The multitaper method gives good estimations of the smoothed spectra.

Then, attenuated seismic traces are created using 200 different random reflectivity series, from which 200 pairs of local reflected waves are obtained to conduct the Q estimation experiment using the two estimation methods. For the noise free case, the estimation results are shown in Figure 36 and 37. We can see that both methods give good estimation results while the result of centroid frequency-shift method is slightly more stable. Next, the two Q estimation methods are further evaluated using reflection data with noise level of $SNR = 4$ and $SNR = 2$. The results are shown in Figure 38 – 41. All these results are comparable. Both methods are insensitive to noise level and gives good estimation results while the centroid frequency-shift method is slightly more stable.

It should point out that, for the match-filter method, the frequency bands for noise attenuation are chosen by SNR level. They can be determined conveniently by evaluating the amplitude spectra of local wavelets. For the centroid frequency-shift method, much narrower frequency bands are used to calculate the centroid frequencies and variances. The mean values of estimation results are sensitive to the chosen frequency range.

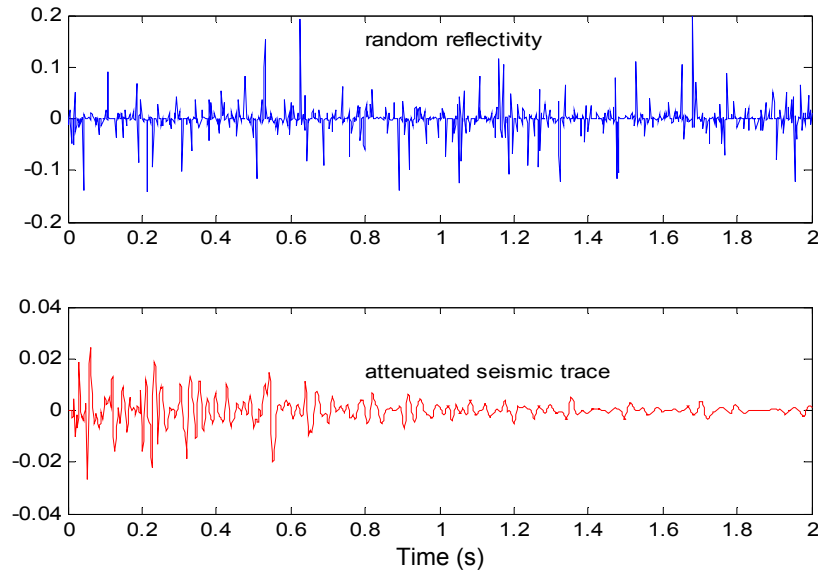


Figure 34. A random reflectivity series (upper). An attenuated seismic trace created using the reflectivity series, a minimum phase wavelet with dominant frequency of 40Hz and a constant Q of 80.

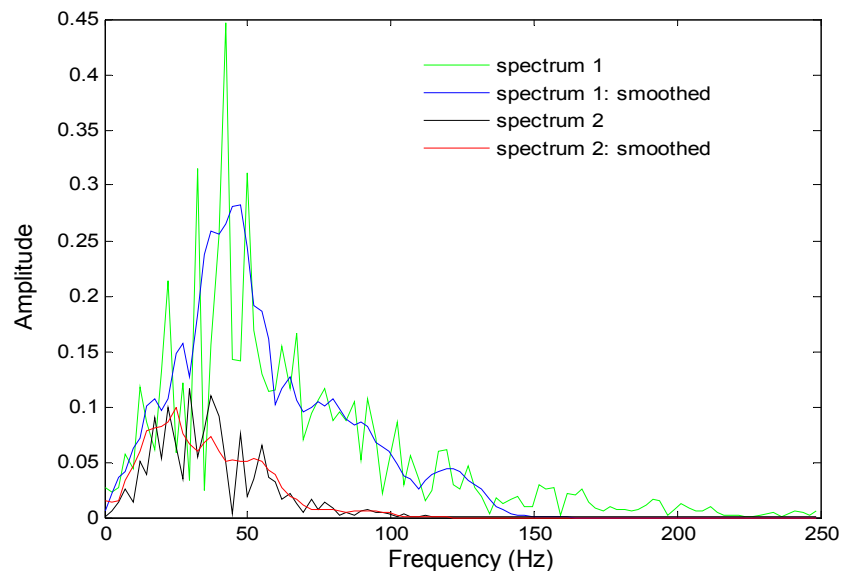


Figure 35. Amplitude spectrum of the 100ms-500ms part of the seismic trace in figure 34 (Green). Amplitude spectrum estimated by multitaper method for the 100ms-500ms part of the seismic trace in figure 34 (Blue). Amplitude spectrum of the 900ms-1300ms part of the seismic trace in figure 34 (Black). Amplitude spectrum estimated by multitaper method for the 900ms-1300ms part of the seismic trace in figure 34 (Red).

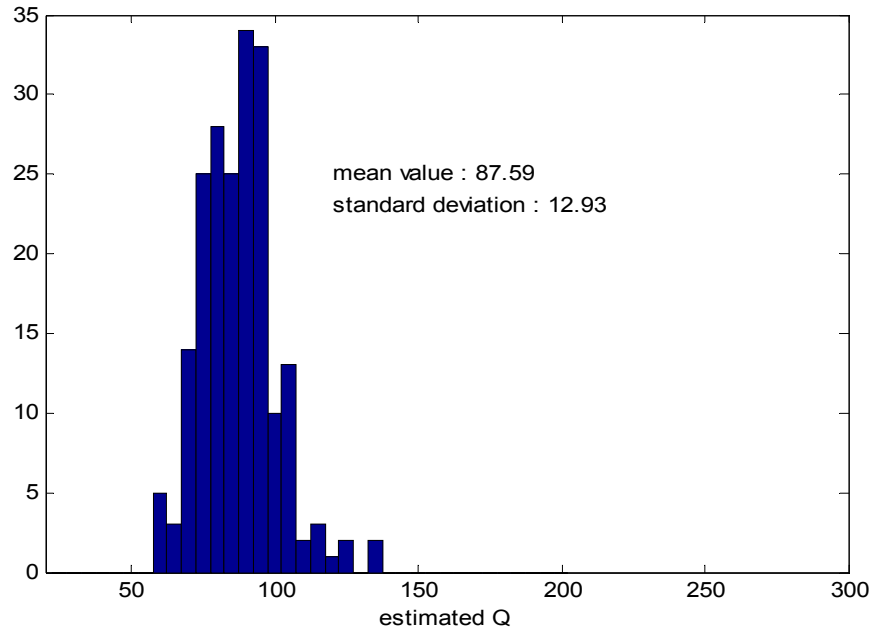


Figure 36. Histogram of the Q values estimated by centroid frequency-shift method using the 100ms-500ms and 900ms-1300ms parts of 200 seismic traces (similar to the one shown in Figure 34) without noise. Both centroid frequencies and variance are estimated from the amplitude spectra of the local wavelets with frequency band of 5Hz – 110Hz and 5Hz – 70Hz respectively.

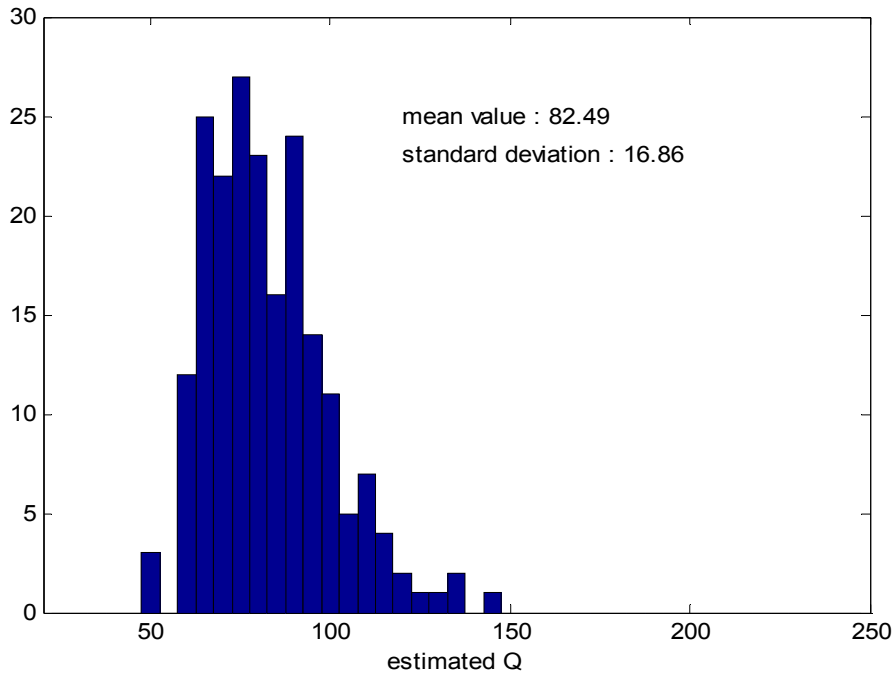


Figure 37. Histogram of the Q values estimated by match-filter method using the 100ms-500ms and 900ms-1300ms parts of 200 seismic traces without noise, which are similar to the one shown in Figure 34.

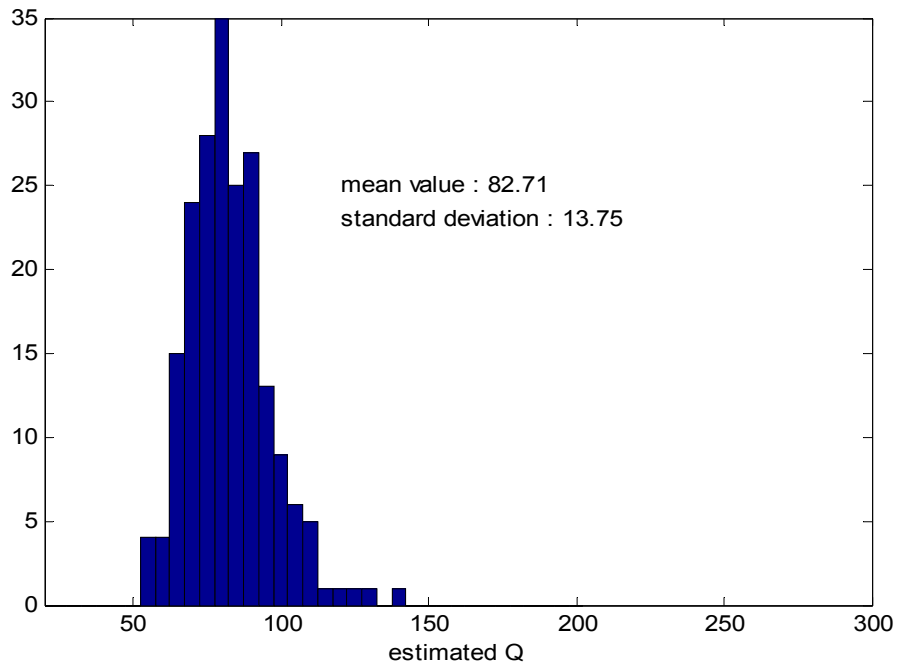


Figure 38. Histogram of the Q values estimated by centroid frequency-shift method using the 100ms-500ms and 900ms-1300ms parts of 200 seismic traces (similar to the one shown in Figure 34) with noise level of SNR=4. Both centroid frequencies and variance are estimated from the amplitude spectra of the local wavelets with frequency band of 5Hz – 100Hz and 5Hz – 65Hz respectively.

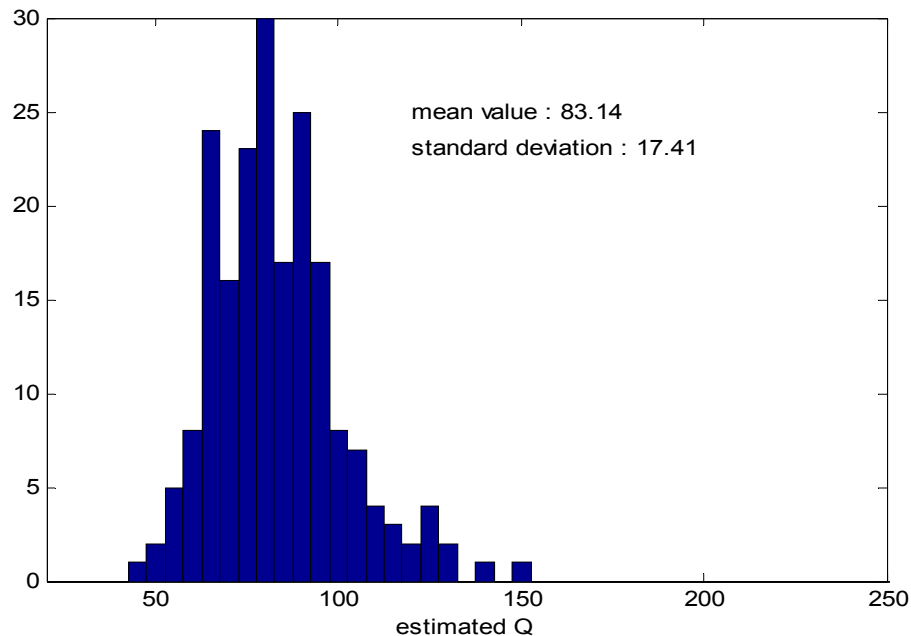


Figure 39. Histogram of the Q values estimated by match-filter method using the 100ms-500ms and 900ms-1300ms parts of 200 seismic traces without noise level of SNR=4, which are similar to the one shown in Figure 34.

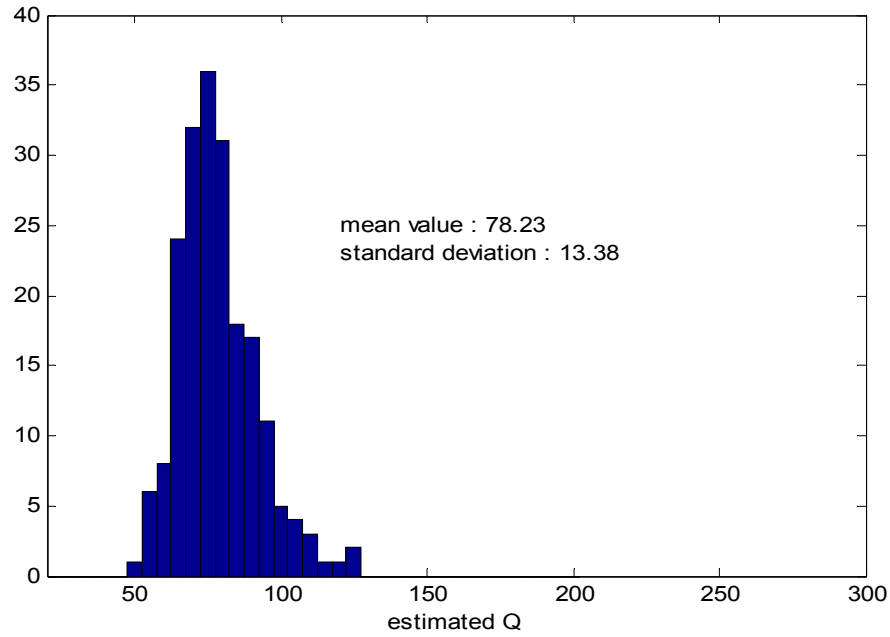


Figure 40. Histogram of the Q values estimated by centroid frequency-shift method using the 100ms-500ms and 900ms-1300ms parts of 200 seismic traces (similar to the one shown in Figure 34) with noise level of SNR=2. Both centroid frequencies and variance are estimated from the amplitude spectra of the local wavelets with frequency band of 5Hz – 95Hz and 5Hz – 60Hz respectively.

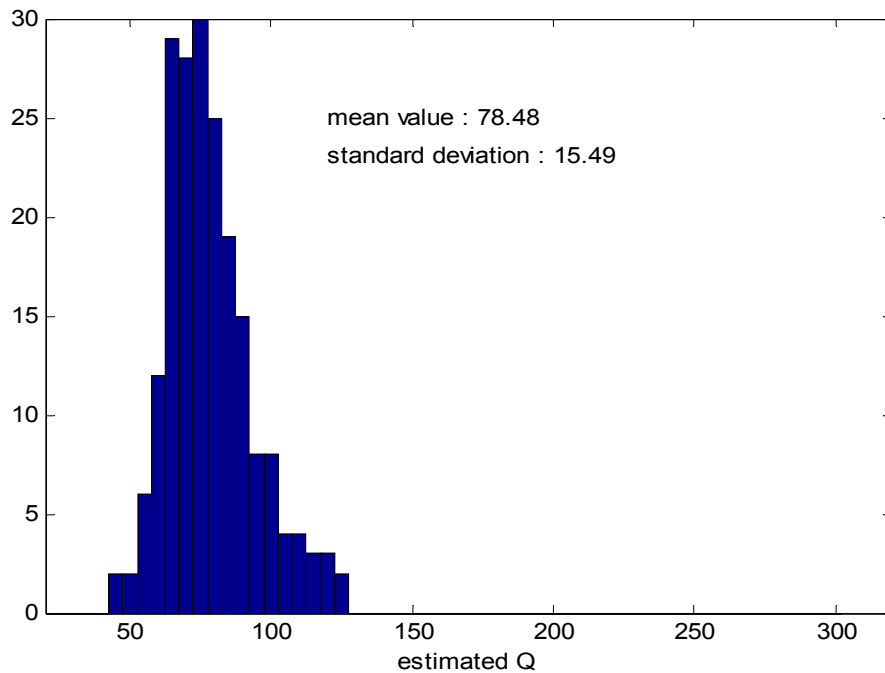


Figure 41. Histogram of the Q values estimated by match-filter method using the 100ms-500ms and 900ms-1300ms parts of 200 seismic traces with noise level of SNR=2, which are similar to the one shown in Figure 34.

Real VSP data

Now, we will use the real VSP data to evaluate the Q estimation methods. Figure 42 shows field zero-offset P-wave VSP data. Since the VSP data consists of downgoing waves and upgoing waves, it is necessary to separate the downgoing waves for Q estimation. First, the first breaks of VSP data are picked and their corresponding time is shown in Figure 43. Linear move out is applied to align the events of VSP data. Then, median filtering is applied to the aligned VSP data for upgoing wave suppression. The downgoing wave VSP data are shown in Figure 44.

When apply complex spectral-ratio method to real data, a practical issue is to choose an appropriate reference frequency f_0 to model the phase difference. One approach is to use the results given by other methods such as classic spectral-ratio method (a special case of complex spectral-ratio method) to calibrate the result of complex spectral-ratio method (only phase information is used for Q estimation). The reference frequency f_0 can be determined by this way. Figure 45 shows the Q estimation result by classic spectral-ratio method using VSP trace 101 and 351. When $f_0 = 22\text{Hz}$, similar result is obtained by complex spectral-ratio method, as shown in Figure 46. Then, with a fixed reference $f_0 = 22\text{Hz}$ and trace interval of 250, Q estimation is conducted for 80 pairs of windowed VSP traces, of which the first pair are the VSP trace 101 and 351 and the last pair are VSP trace 180 and 430. The Q -estimation results are shown in Figure 47. We can see that the complex ratio-method (only phase information employed) gives unreasonable results at some cases. Another approach is to choose f_0 by a least-squares error solution to the modeled phase difference and the computed phase difference. The Q -estimation results for the 80 pairs of VSP traces are shown in Figure 48, and the corresponding reference frequencies are shown in Figure 49. We can see that the estimated Q values are more stable than results shown in Figure 47, while they have significant variations. We also can see that the reference frequencies vary significantly, which may not be physically true. Generally, both approaches do not work for the real data, which may indicates that the phase difference between wavelets is distorted during the propagation and is not suitable to be approximated by the phase of a minimum phase wavelet. To make the complex spectral-ratio method applicable, minimum-phase equivalent wavelets are computed before Q estimation for the VSP traces. Then, with the calibration from classic spectral-ratio method, a reference frequency $f_0 = 600\text{Hz}$ is chosen to model the phase difference. The Q -estimation results are shown in Figure 50, which are stable and similar to the results given by the classic spectral ratio method.

Using the 80 pairs of windowed VSP traces described above, we can evaluate the centroid frequency-shift method, classic spectral ratio method (reduced complex spectral-ratio method), and match-filter method. The multitaper methods are used to smooth the amplitude spectra for all these three methods. Figure 51 shows the amplitude spectra of the first pair of local wavelets. For the centroid frequency-shift method, frequency bands of 5Hz-100Hz and 5Hz-70Hz are used to estimate the centroid frequencies and variances. For the spectral-ratio method, the straight line fitting is conducted over 15Hz - 70Hz. For the match-filter method, frequency bands of 10Hz - 150Hz and 10Hz - 120Hz are used to band filtering the random noise. The estimation results are shown in Figure 52. We can see that the results of spectral-ratio method and match-filter method are

consistent, while the result of centroid frequency-shift method are significantly deviated from them.

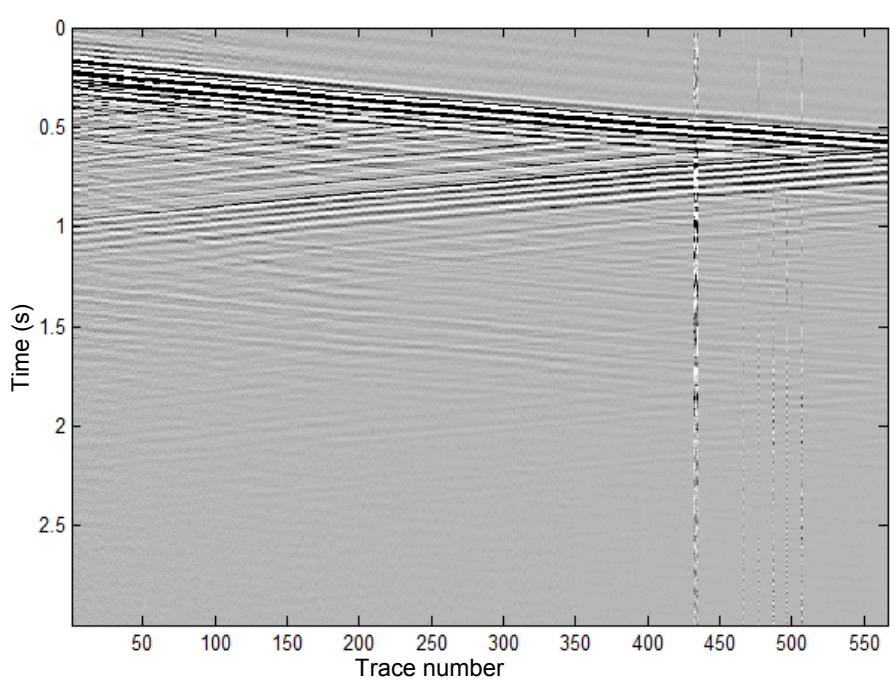


Figure 42. Ross Lake VSP data (vertical component P-wave).

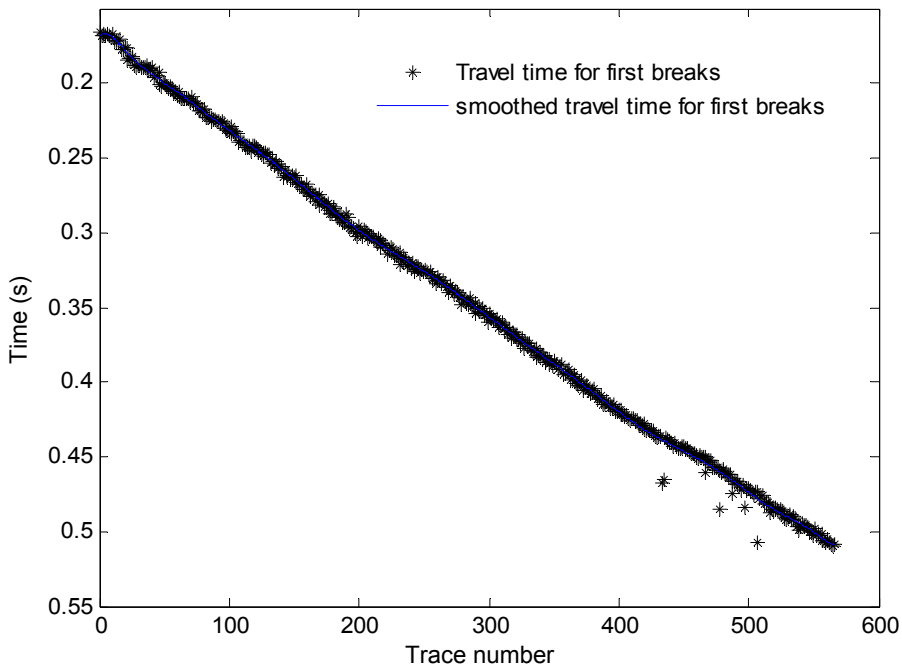


Figure 43. First breaks of VSP data shown in figure 52.

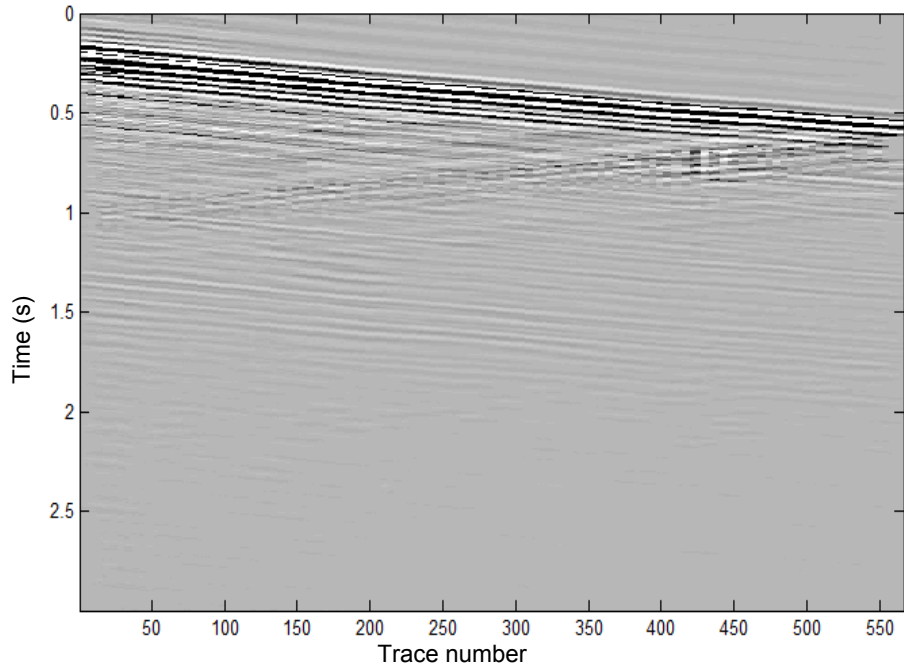


Figure 44. VSP data with upgoing wave suppression.

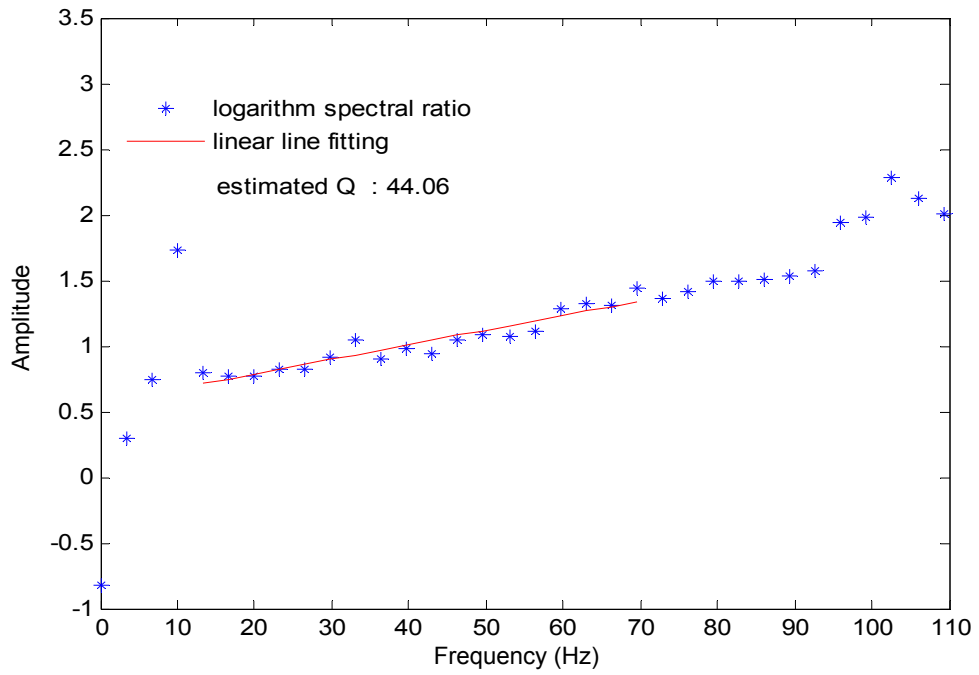


Figure 45. Q estimation by classic spectral-ratio method using of VSP traces 102 and 352 shown in Figure 44.

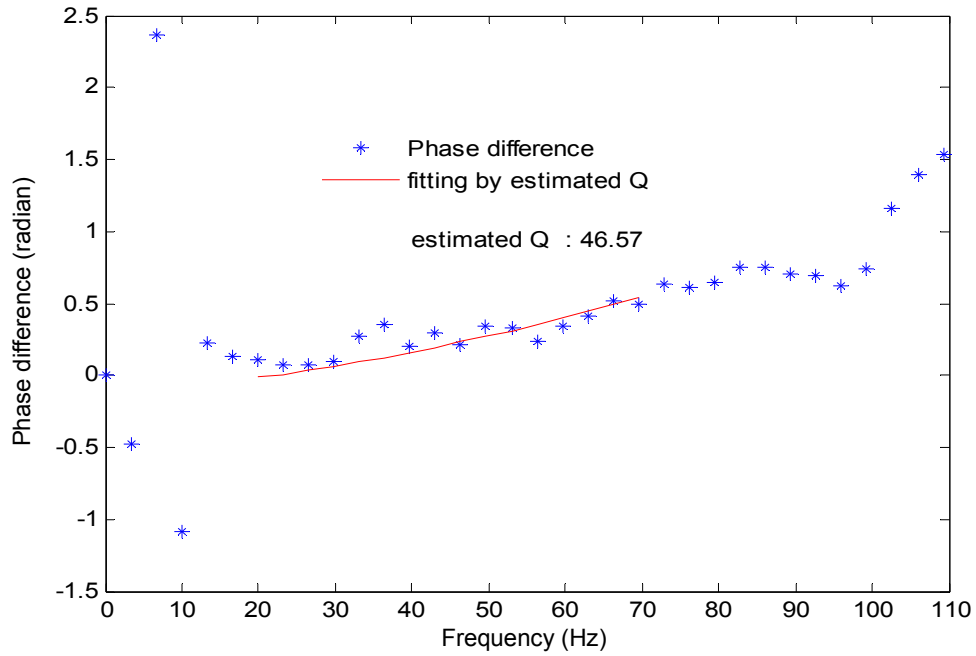


Figure 46. Q estimation by complex spectral-ratio method with only phase information employed (reference frequency $f_0 = 22\text{Hz}$) using of VSP traces 102 and 352 shown in Figure 44.

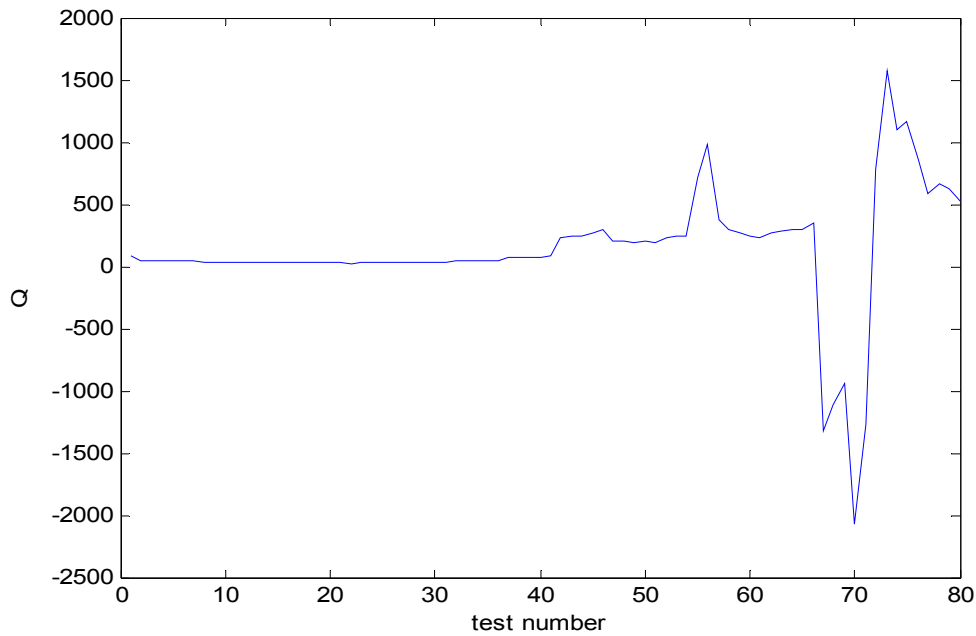


Figure 47. Q estimation by complex spectral-ratio method with only phase information employed (reference frequency $f_0 = 22\text{Hz}$), using 80 pairs of VSP traces shown in Figure 44 (Each pair has a fixed trace interval of 250; the first pair are the VSP trace 101 and 351 and the last pair are VSP trace 180 and 430).

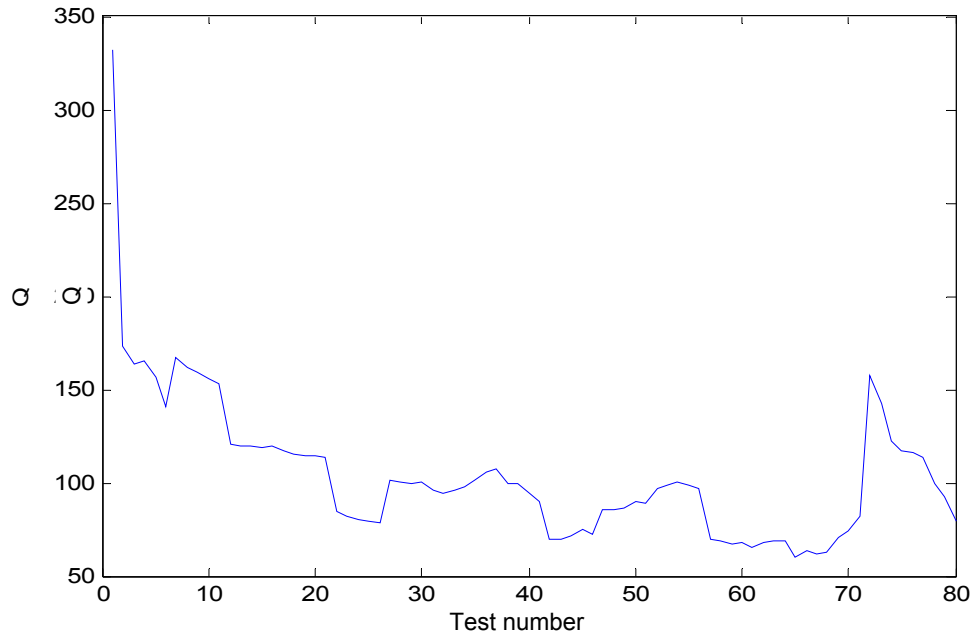


Figure 48. Q estimation by complex spectral-ratio method with only phase information employed (reference frequency is chosen by a least-square minimization approach), using 80 pairs of VSP traces shown in Figure 44 (Each pair has a fixed trace interval of 250; the first pair are the VSP trace 101 and 351 and the last pair are VSP trace 180 and 430).

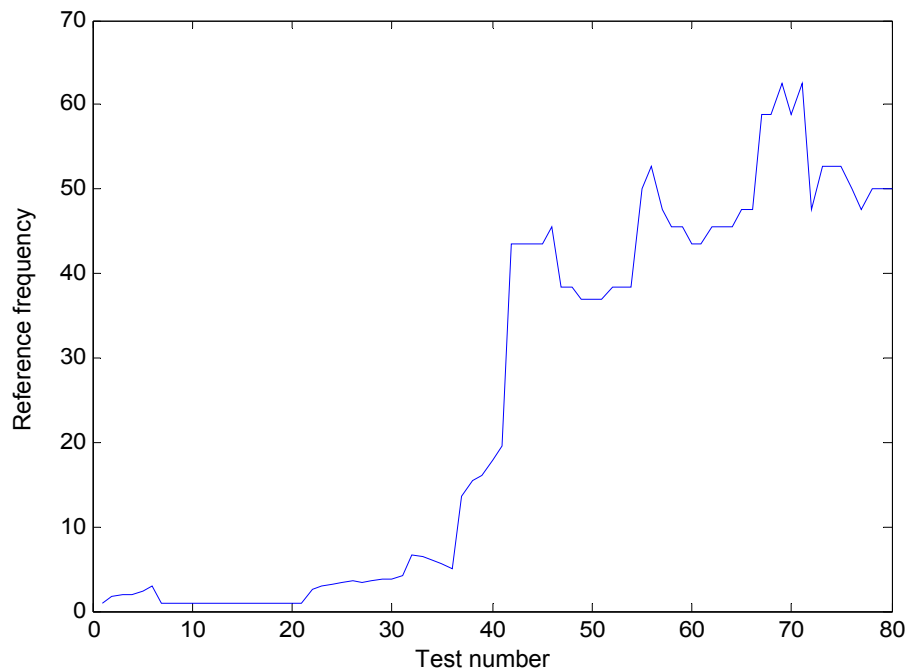


Figure 49. The chosen reference frequencies corresponding to the test shown in Figure 48.

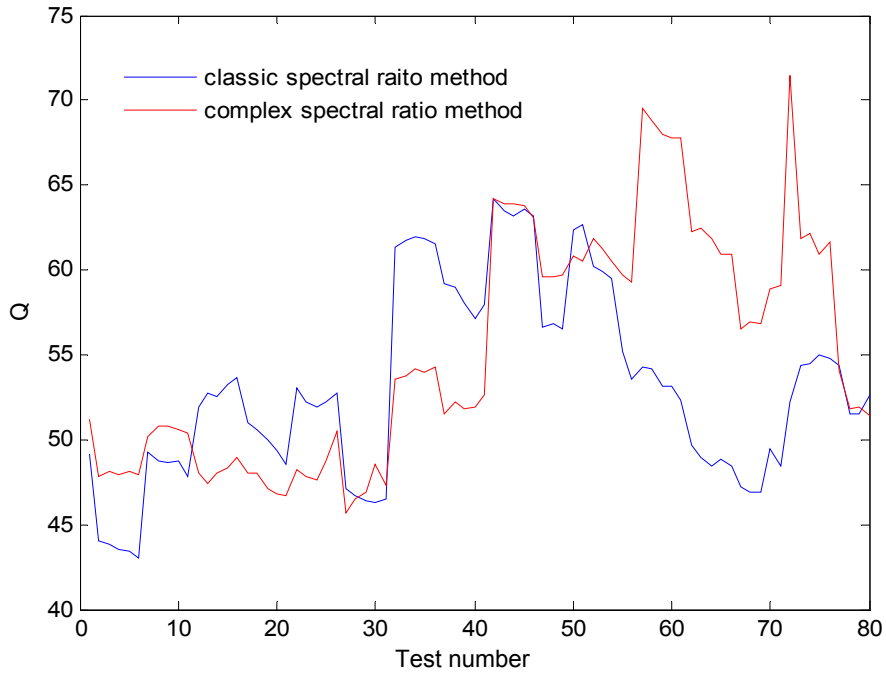


Figure 50. Q estimation by complex spectral-ratio method with only phase information employed (reference frequency $f_0 = 600\text{Hz}$), using 80 pairs of VSP traces shown in Figure 44(Each pair has a fixed trace interval of 250; the first pair are the VSP trace 101 and 351 and the last pair are VSP trace 180 and 430). Minimum-phase equivalent wavelets are computed before Q estimation for the VSP traces.

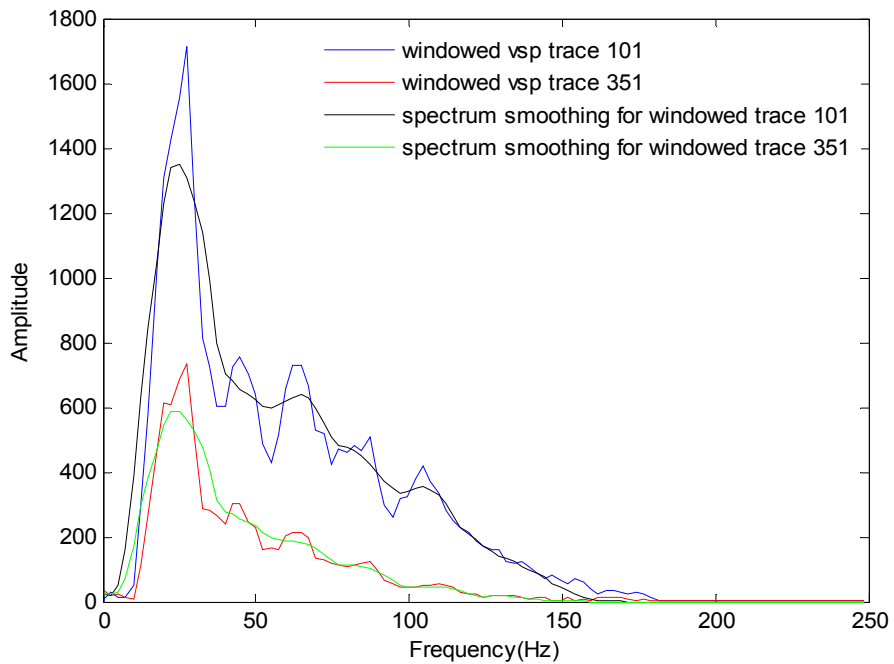


Figure 51. Amplitude spectra of the windowed VSP trace 101 and 351.

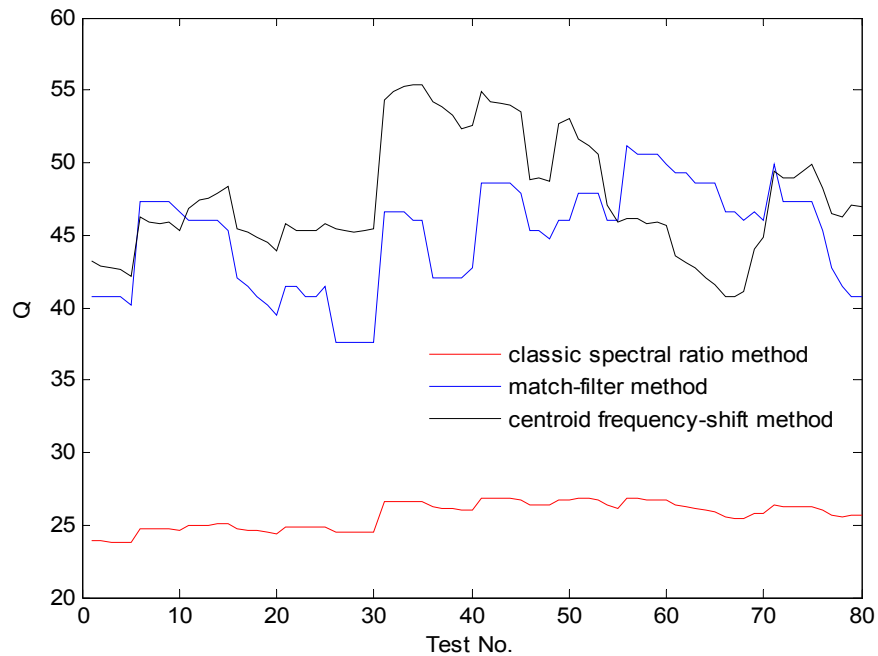


Figure 52. Q estimation by classic spectral-ratio method, centroid frequency-shift method and match-filter method using 80 pairs of VSP traces shown in Figure 44 (Each pair has a fixed trace interval of 250; the first pair are the VSP trace 101 and 351 and the last pair are VSP trace 180 and 430)

CONCLUSION AND DISCUSSION

The relative performances of complex spectral-ratio method, centroid frequency-shift method, and match-filter method are evaluated in this paper. Testing results show that all these methods are robust to noise. The centroid frequency-shift method and match-filter method are suitable for application to reflection data.

With the employment of phase information, the complex spectral-method can obtain better estimation result than the classic spectral-method. However, it is subject to the reference frequency chosen for modeling phase difference as well. Inaccurate reference frequency can distort the estimation. To apply the complex spectral-ratio method to real data, minimum phase equivalent wavelet transformation are necessary before Q estimation, and the chosen of reference frequency can be chosen with the calibration of other methods.

For the centroid frequency-shift method, it is derived from the case that the original amplitude spectrum of local wavelet is Gaussian. Even for the ideal case, it gives an approximate estimation. If a broad frequency band is used to calculate the centroid frequency and variance, it may give obviously deviated and unstable result. Choosing a limited frequency range for the calculation can improve the estimation in two ways. First, with a limited frequency range, the calculation of centroid frequency and variance can be more stable. Second, within the chosen frequency band, the amplitude spectrum of local wavelet can be better approximate by Gaussian, which makes the relation between attenuation and centroid frequency-shift more accurate. However, the estimated result

might be sensitive the chosen frequency band, since it is directly proportional to the calculated frequency shift and variance. In addition, it seems that there is no convenient way to determine an appropriate frequency band to optimize the estimation result.

The match-filter method gives accurate and stable estimation result for both VSP data and reflection data. Theoretically, it is subject to the frequency bands used to filtering the local wavelets for noise attenuation. The associated frequency bands can be determined by evaluating the SNR level of local wavelets with convenience.

ACKNOWLEDGEMENTS

We would like to thank the sponsors of CREWES project for their financial support.

REFERENCES

- Aki K. and Richard P. G., 1980, Quantitative Seismology, W. H. Freeman and Co., San Francisco.
- Balis, E., 2011, Q-factor estimation through optimization approach to near-offset VSP data: SEG 2011 annual meeting
- Bath, M., 1974, Spectral analysis in geophysics: Developments in Solid Earth Geophysics, Vol 7, Elsevier Science Publishing Co.
- Cheng, P., and Margrave, G. F., 2009, Q analysis using synthetic viscoacoustic seismic data: CREWES research report, 21.
- Cheng, P., and Margrave, G. F., 2012a, A match-filter method for Q estimation: SEG expanded abstract, SEG 2012 annual meeting.
- Cheng, P., and Margrave, G. F., 2012b, Estimation of Q: a comparison of different computational methods: CREWES research report, 24.
- Engelhard, L., 1996, Determination of the seismic wave attenuation by complex trace analysis: Geophysical Journal International, 125, 608-622.
- Futterman, W. I., 1962, Dispersive body waves: J. Geophys. Res., 67, 5279-5291
- Jannsen, D., Voss, J., and Theilen, F., 1985, Comparison of methods to determine Q in shallow marine sediments from vertical reflection seismograms: Geophysical Prospecting, 33, 479-497, 1985.
- Hauge, P. S., 1981, Measurements of attenuation from vertical seismic profiles: Geophysics, 46, 1548-1558.
- Margarve G. F., 1998, Theory of nonstationary linear filtering in the Fourier domain with application to time-variant filtering: Geophysics, 63, 244-259
- Neep, J. P., Sams, M. S., Worthington, M. H., and O'Hara-Dhand, K. A., 1996, Measurement of seismic attenuation from high-resolution crosshole data: Geophysics, 61, 1175-1188.
- Park, J., Lindberg, C. R., and Vernon III, F. L., 1987, Multitaper spectral analysis of high frequency seismograms: J. Geoph. Res., 92, 12 675-12 684.
- Patton, S. W., 1988, Robust and least-squares estimation of acoustic attenuation from well-log data: Geophysics, 53, 1225-1232.
- Quan, Y., and Harris, J. M., 1997, Seismic attenuation tomography using the frequency shift method: Geophysics, 62, 895-905.
- Raikes, S. A., and R. E. White, 1984, Measurements of earth attenuation from downhole and surface seismic recordings: Geophysical Prospecting, 32, 892-919.
- Sheriff, R. E., and L. P. Geldart, 1995, Exploration seismology, 2nd ed.: Cambridge University Press.
- Sun, X., X. Tang, C. H. Cheng, and L. N. Frazer, 2000, P- and S- wave attenuation logs from monopole sonic data: Geophysics, 65, 755-765.
- Thomson, D. J., 1982, Spectrum estimation and harmonic analysis: Proc. IEEE, 70, 1055-1096.
- Tonn, R., 1991, The determination of seismic quality factor Q from VSP data: A comparison of different computational methods: Geophys. Prosp., Vol. 39, 1-27.
- White, R. E., 1992, The accuracy of estimating Q from seismic data: Geophysics, 57, 1508-1511.